



## Abstract

The relationship between phytoplankton assemblages and the associated optical properties of the water body is important for the further development of algorithms for large-scale remote sensing of phytoplankton biomass and the identification of phytoplankton functional types (PFTs), which are often representative for different biogeochemical export scenarios. Optical in-situ measurements aid in the identification of phytoplankton groups with differing pigment compositions and are widely used to validate remote sensing data. In this study we present results from an interdisciplinary cruise aboard the R/V *Polarstern* along a north-to-south transect in the eastern Atlantic Ocean in November 2008. Phytoplankton community composition was identified using a broad set of in-situ measurements. Water samples from the surface and the depth of maximum chlorophyll concentration were analyzed by high performance liquid chromatography (HPLC), flow cytometry, spectrophotometry and microscopy. Simultaneously, the above- and underwater light field was measured by a set of high spectral resolution (hyperspectral) radiometers. An unsupervised cluster algorithm applied to the measured parameters allowed us to define bio-optical provinces, which are compared to ecological provinces proposed elsewhere in the literature. This method has the potential to become an automated approach where satellite data could be used to identify shifting boundaries of established ecological provinces or to track exceptions from the rule to improve our understanding of the biogeochemical cycles in the ocean.

## 1 Introduction

Marine phytoplankton stands at the base of most marine food webs and contributes significantly to global primary production. Chlorophyll-*a* (Chl-*a*) concentration as a proxy for phytoplankton biomass and primary production can be monitored on a global scale through remote sensing of ocean colour (Carr et al., 2006; McClain, 2009; Saba et al., 2011). However, the phytoplankton community is composed of thousands of species

**BGD**

8, 7165–7219, 2011

## Bio-optical provinces in the eastern Atlantic Ocean

B. B. Taylor et al.

Title Page

Abstract

Introduction

Conclusions

References

Tables

Figures

◀

▶

◀

▶

Back

Close

Full Screen / Esc

Printer-friendly Version

Interactive Discussion



which differ significantly in their role in the ecosystem. The use of bulk Chl-*a* distribution only as a general proxy for phytoplankton biomass bears the risk of considerable errors as it does not differentiate between the various functional groups of phytoplankton. It might also involve biases as Chl-*a* concentration is not always proportional to biomass (Marañón et al., 2000). Given that some pigments are characteristic of certain phytoplankton groups, inventories of these pigments have been used to determine the approximate abundance of these phytoplankton functional groups (PFTs) (e.g. Letelier et al., 1993; Mackey et al., 1996; Vidussi et al., 2001; Bricaud et al., 2004; Jeffrey et al., 2005). Although the use of pigments to determine phytoplankton groups can also bear the risk of errors through the gross simplification of assigning one specific pigment to one group of algae, we believe that the results still give a good approximation of the true phytoplankton composition. It is a method which allows for higher analysis frequency than looking at each sample through the microscope. Furthermore it permits the analysis of a broader range of cell-sizes including the large diatoms, which are too big for flow cytometric analysis as well as the small-celled species such as *Synechococcus* and prochlorophytes which are too small to be identified by microscopy. The importance of pico-prokaryotes and -eukaryotes in the marine carbon cycle has been shown frequently in the last three decades for the tropical Atlantic (e.g. Agustí and Duarte, 1999; Zubkov et al., 2000; Marañón et al., 2001; Barlow et al., 2002; Veldhuis and Kraay, 2004).

In this study, pigment composition forms the basis to group the samples by means of an unsupervised clustering analysis, which is subsequently applied to all other bio-optical data sets. We use hyperspectral field data of inherent optical properties (IOPs) such as particulate absorption, and apparent optical properties (AOPs) such as remote sensing reflectance to define ecological units on a north-to-south transect across the eastern Atlantic Ocean. Flow cytometric and microscopic measurements as well as oceanographic data provide additional information to characterize the clusters.

On land, the distinction between different ecosystems such as the edge of a forest or the extent of a desert is generally easier compared to the marine environment. Due

**BGD**

8, 7165–7219, 2011

## Bio-optical provinces in the eastern Atlantic Ocean

B. B. Taylor et al.

Title Page

Abstract

Introduction

Conclusions

References

Tables

Figures

◀

▶

◀

▶

Back

Close

Full Screen / Esc

Printer-friendly Version

Interactive Discussion



to the highly dynamic nature of the oceans and the lack of knowledge about many of those dynamics, these boundaries between ecological units are much harder to observe. They are, however, no less real (Sathyendranath et al., 1995; Platt and Sathyendranath, 1999; Hooker et al., 2000; Li and Harrison, 2001; Devred et al., 2007; Longhurst, 2007). Areas in the world's oceans with similar physical and biological characteristics are generally referred to as ecological or biogeochemical provinces or units (e.g. Platt et al., 2005). Partitioning the ocean into provinces can assist us in understanding complex patterns in the oceans and helps us to extrapolate measured parameters such as primary production or carbon cycling over large spatial scales (Platt et al., 2005; Barlow et al., 2007; Longhurst, 2007). The approximation of ecological parameters (e.g. in modelling or in the interpretation of satellite data) can be more accurate if we know which areas exhibit similar dynamics.

Several studies have used Chl-*a* as one of the descriptors to define marine ecological provinces (e.g. Devred et al., 2007; Hardman-Mountford et al., 2008). Here, we use pigment composition in conjunction with hyperspectral optical data to establish an ecological geography of the eastern Atlantic Ocean. In light of the recent advances in hyperspectral technology on the remote sensing observing platforms, the possibility of characterizing marine ecological units and phytoplankton communities through hyperspectral measurements becomes increasingly interesting and important. These methods will help to further assess the extension and dynamic of ecological provinces in the ocean on a large spatial and temporal scale. Finally, we compare our bio-optical units to biogeochemical provinces previously proposed by Longhurst (2007).

**BGD**

8, 7165–7219, 2011

## Bio-optical provinces in the eastern Atlantic Ocean

B. B. Taylor et al.

Title Page

Abstract

Introduction

Conclusions

References

Tables

Figures

◀

▶

◀

▶

Back

Close

Full Screen / Esc

Printer-friendly Version

Interactive Discussion



## 2 Methods

### 2.1 In-situ sample and data collection

#### 2.1.1 Sample collection

Samples were collected at 48 stations, of which 26 were CTD stations, during the ANT XXV-1 expedition of the R/V *Polarstern* in November 2008 along a north-to-south transect through the eastern Atlantic Ocean from Bremerhaven (Germany) to Cape Town (South Africa) (Fig. 1). At the 22 stations without CTD casts only surface waters were sampled through the moonpool of the ship. The CTD stations were performed once a day at noon local time and involved CTD casts with water samplers as well as measurements of remote sensing reflectance. Measurements of surface salinity, temperature and fluorescence were conducted continuously throughout the cruise and are described in more detail below. Water samples for pigment and absorption analysis were filtered on GF/F filters, shock-frozen in liquid nitrogen and stored at  $-80^{\circ}\text{C}$ . Samples for flow cytometry were preserved with 0.1 % glutaraldehyde (final concentration), shock-frozen in liquid nitrogen and stored at  $-80^{\circ}\text{C}$  (Marie et al., 2005).

#### 2.1.2 CTD profiles and continuous data from onboard ship devices

Temperature, salinity and Chl-*a* profiles were determined using a Seabird 911 Plus CTD with a Wetlabs ECO FL fluorometer fitted to a rosette system provided with 24 × 12l Niskin bottles. Density was calculated from salinity and temperature data and mixed layer depth ( $Z_m$  (sigma)) was derived from density profiles using the definition from Levitus (1982), where  $Z_m$  is defined as the depth at which a change from the surface density of 0.125 has occurred. Continuous temperature and salinity data were recorded with the onboard thermosalinograph SEABIRD SBE 21 equipped with an external thermometer SBE 38 installed at the bow of the ship (Rohardt, 2009). The data set was processed according to Fahrbach et al. (2007).

**BGD**

8, 7165–7219, 2011

## Bio-optical provinces in the eastern Atlantic Ocean

B. B. Taylor et al.

Title Page

Abstract

Introduction

Conclusions

References

Tables

Figures

◀

▶

◀

▶

Back

Close

Full Screen / Esc

Printer-friendly Version

Interactive Discussion



### 2.1.3 Radiometric measurements

Underwater optical light fields were measured with hyperspectral radiometers (RAM-SES, TriOS GmbH, Germany) measuring profiles of radiance and irradiance. The instruments cover a wavelength range of 320 nm to 950 nm with an optical resolution of 3.3 nm and a spectral accuracy of 0.3 nm. All measurements were collected with sensor-specific automatically adjusted integration times (between 4 ms and 8 s).

A total of 22 radiometric profiles were collected simultaneously with the CTD profiles at noon down to a maximum depth of 190 m, with a radiance sensor measuring upwelling radiance ( $L_u$ ), and irradiance sensor measuring downwelling irradiance ( $E_d$ ). Irradiance at the surface ( $E_d^+$ ) was measured as a reference with a third sensor placed above-water and allowed normalization of the in-water measurements according to Stramski et al. (2008). One of the in-water sensors was equipped with an inclination and a pressure sensor. To avoid ship shadow, the ship was oriented such that the sun was illuminating the side where the measurements were taking place.

All radiometric data were checked for minimum incoming solar light or precipitation (Wernand, 2002). The pitch and roll data measured by the ship must not exceed values larger than  $5^\circ$ . For the in-water data, the inclination in either dimension had to be smaller than  $14^\circ$  (Matsuoka et al., 2007). The profile data were averaged in discrete intervals of 2 m down to a depth of 48 m, 4 m for depths between 48 and 80 m and 10 m for all measurements below 80 m. As surface waves strongly affect measurements in the upper few meters, deeper measurements that are more reliable had to be used and extrapolated to the sea surface (Mueller et al., 2003). Similar to Stramski et al. (2008) a depth interval was defined ( $z' = 7$  to 21 m) to calculate the vertical attenuation coefficients for downwelling irradiance and upwelling radiance, (i.e.  $K_d(\lambda, z')$  and  $K_u(\lambda, z')$ , respectively). With  $K_d(\lambda, z')$  and  $K_u(\lambda, z')$ , the subsurface irradiance  $E_d^-(\lambda, 0 \text{ m})$  and radiance  $L_u^-(\lambda, 0 \text{ m})$  were extrapolated from the profiles of  $E_d(\lambda, z)$  and  $L_u(\lambda, z)$ . For the calculation of the remote sensing reflectance ( $R_{rs}(\lambda)$ ), the subsurface  $L_u^-(\lambda, 0 \text{ m})$  was propagated through the water-air interface by applying a transfer coefficient of 0.5425

**BGD**

8, 7165–7219, 2011

## Bio-optical provinces in the eastern Atlantic Ocean

B. B. Taylor et al.

Title Page

Abstract

Introduction

Conclusions

References

Tables

Figures

◀

▶

◀

▶

Back

Close

Full Screen / Esc

Printer-friendly Version

Interactive Discussion



determined by Stramski et al. (2008) for the same geographical area.  $R_{rs}(\lambda)$  was therefore calculated using the above-water reference downwelling irradiance  $E_d^+(\lambda)$ :

$$R_{rs}(\lambda) = (0.5425 \cdot L_u^-(\lambda, 0 \text{ m})) / E_d^+(\lambda)$$

$E_d(\text{PAR}, z)$  profiles were calculated as the integral of  $E_d(\lambda, z)$  for all wavelengths from 400 nm to 700 nm for each depth interval. To determine the euphotic depth,  $Z_{eu}$ , the natural logarithm of  $E_d(\text{PAR}, z)$  was fitted linearly with  $z$ :

$$E_d'(\text{PAR}, z') = \exp(m \cdot z' + n) \quad (\text{with fit parameters } m \text{ and } n)$$

$z'$  varied in steps of 1 cm from 0 m to 200 m depth. The euphotic depth was then calculated from

$$0.01 = E_d'(\text{PAR}, Z_{eu}) / E_d'(\text{PAR}, 0 \text{ m})$$

#### 2.1.4 Continuous fluorescence measurements by Fast Repetition Rate fluorimetry (FRRf)

Variable fluorescence was measured continuously with a FastTracka I fluorimeter (Chelsea, West Molesey, UK) in the ship's moonpool at 11 m depth using water pumped through the dark chamber of the instrument by a peristaltic pump. The minimum fluorescence (F0) measurements were used as an indicator for total Chl-*a* concentration (TChl-*a*), as F0 is correlated to the amount of available TChl-*a* pigments (Kolber et al., 1998).

For further analysis, the FRRf measurements were averaged to 10 min intervals. The F0 data taken during daylight were corrected for photochemical quenching by the method developed by Strass (1990). The surface F0 daytime measurements were corrected for the quench due to light in the surface waters by comparing them to the global radiation data measured by the ship's system. Generally, it can be seen – if values are not too low – that F0 values decrease during daylight due to non-photochemical quenching. The mean of the light measurements during one day was subtracted from

**BGD**

8, 7165–7219, 2011

## Bio-optical provinces in the eastern Atlantic Ocean

B. B. Taylor et al.

Title Page

Abstract

Introduction

Conclusions

References

Tables

Figures

◀

▶

◀

▶

Back

Close

Full Screen / Esc

Printer-friendly Version

Interactive Discussion



the mean of the dark measurements of the corresponding day. The resulting offset was added to the day time measurements. In general, day time quenching was low except for areas with Chl-*a* concentration above 0.5 mg m<sup>-3</sup> where the effect was more pronounced.

Based on the pigment-based clusters identified by the statistical analysis described below, the F0 data for each cluster were calibrated with the Chl-*a* concentrations derived from the HPLC analysis (see Sect. 2.2.1). In particular, different Chl-*a* conversion factors were calculated for each cluster by comparing the collocated F0 data to the HPLC TChl-*a* value. Using the conversion factor specific for each cluster, the continuous surface TChl-*a* concentrations were calculated from the F0 data.

## 2.2 Sample analysis

### 2.2.1 Pigment analysis

Pigment composition was analysed by High Performance Liquid Chromatography (HPLC) following a method described in Hoffmann et al. (2006) adjusted to our instruments. In short, samples were measured using a Waters 600 controller combined with a photodiode array detector (PDA, Waters 2998) and an auto sampler (Waters 717plus). For solvents and solvent gradient see Table 1. As an internal standard, 100 µl canthaxanthin (Roth) was added to each sample. Identification and quantification of the different pigments were carried out using the program EMPOWER by Waters. A list of the pigments used for this study, their abbreviations and their associated phytoplankton groups can be found in Table 2.

### 2.2.2 Absorption measurements

Measurements of the particulate absorption were carried out on a dual-beam UV/VIS spectrophotometer (Cary 4000, Varian Inc.) equipped with a 150 mm integrating sphere (external DRA-900, Varian, Inc. and Labsphere Inc., made from Spectralon

**BGD**

8, 7165–7219, 2011

## Bio-optical provinces in the eastern Atlantic Ocean

B. B. Taylor et al.

Title Page

Abstract

Introduction

Conclusions

References

Tables

Figures

◀

▶

◀

▶

Back

Close

Full Screen / Esc

Printer-friendly Version

Interactive Discussion



(TM)) using a quantitative filterpad technique modified as follows (see e.g. Simis et al., 2005). The filters were placed in the center of the integrating sphere using a center-mount filter holder perpendicular to the light beam. A wavelength scan from 300 to 850 nm with a resolution of 1 nm (slit width 2 nm, scan rate 150 nm min<sup>-1</sup>) was performed, when the reflectance ports were covered with Spectralon(TM) reflectance standards. The baseline was recorded beforehand with a clean, dry filter, and a filter which was soaked for more than 30 min in purified water served as a reference. The absorption coefficient was calculated from optical density (OD) measurements using a path length amplification factor of 4.5 ( $\beta = 1/4.5$ , R. Röttgers, personal communication, 2011) as  $a [m^{-1}] = -\ln(T) \cdot A \cdot \beta / V$ , where the transmittance  $T = \exp(-OD)$ ,  $V$  is the filtrated sample volume in m<sup>3</sup> and  $A$  the filter clearance area in m<sup>2</sup>. Results from the original filter gave particulate absorption,  $a_p$ . To determine the absorption by non-algal particles ( $a_{NAP}$ ), the algal pigments were bleached with NaOCl as described in Tassan and Ferrari (1995) and Ferrari and Tassan (1999). The bleached filters were measured as described above. To obtain the particulate absorption of phytoplankton ( $a_{ph}(\lambda)$ )  $a_{NAP}$  was subtracted from  $a_p$ .

### 2.2.3 Flow cytometry

Phytoplankton cells were enumerated from preserved and frozen, unstained samples by using their specific Chl-*a* and phycoerythrin autofluorescence according to Marie et al. (2005). Both Chl-*a* and phycoerythrin are excited with the common 488-nm excitation line and fluoresce at 690 nm (red) and 570 nm (orange), respectively. Flow cytometry was performed on a FACScalibur with an excitation beam of 488 nm, two light scatter detectors at 180° (forward scatter) and at 90° (side scatter) and several photomultipliers detecting at 530 nm (beads), 585 nm (orange fluorescence) and 670 nm (red fluorescence). Phytoplankton groups were separated according to their red and orange fluorescence and scattering characteristics. Yellow-green Fluoresbrite<sup>®</sup> Microspheres with a diameter of 1 μm (Polysciences) were used as an internal standard. The data were analysed with the instrument software “CellQuest”.

**BGD**

8, 7165–7219, 2011

## Bio-optical provinces in the eastern Atlantic Ocean

B. B. Taylor et al.

Title Page

Abstract

Introduction

Conclusions

References

Tables

Figures

◀

▶

◀

▶

Back

Close

Full Screen / Esc

Printer-friendly Version

Interactive Discussion



## 2.2.4 Microscopy

Samples were fixated with 2% buffered formaldehyde (end concentration) and stored in brown glass bottles in a dark, cool and dry place. For analysis, the samples were introduced into a settling chamber and the phytoplankton was allowed to settle for 48 h. Phytoplankton cells were then identified and counted by the Utermöhl method (Utermöhl, 1958; Edler, 1979) using a Zeiss IM35 inverted microscope equipped with phase contrast and 400× magnification.

## 2.3 Data analysis

### 2.3.1 Interpretation of pigment data

Some pigments have been used in the past as marker pigments for one specific phytoplankton group. Table 2 lists the pigments analysed in this study, their abbreviations, which will be used in the text and the phytoplankton groups to which some diagnostic pigments have been assigned (see references in the table). Two methods were applied to interpret the pigment data. Firstly, phytoplankton size classes were calculated by a procedure proposed by Vidussi et al. (2001), which was subsequently refined by Uitz et al. (2006). The relative proportions of microphytoplankton (20–200 µm), nanophytoplankton (2–20 µm) and picophytoplankton (<2 µm) were estimated from the concentrations of 7 diagnostic pigments.

The general assumptions are

- Fuco and Peri are diagnostic pigments for diatoms and dinoflagellates, respectively, which dominate the microplankton (>20 µm),
- Allo, 19 BF and 19 HF characterize the nanoplankton (2–20 µm),
- Picoplankton (<2 µm) is assessed from Zea and total Chl-*b* (TChl-*b*)

**BGD**

8, 7165–7219, 2011

## Bio-optical provinces in the eastern Atlantic Ocean

B. B. Taylor et al.

Title Page

Abstract

Introduction

Conclusions

References

Tables

Figures

◀

▶

◀

▶

Back

Close

Full Screen / Esc

Printer-friendly Version

Interactive Discussion





distance between all samples included in the input data set. In this study, an angular distance was utilized when the similarity was computed between pairs of spectra because it reflects better the differences in the spectral shape of optical data. This approach is particularly interesting in our case due to the focus on spectral features related to the specific pigment composition.

The feasibility of using hyperspectral optical data for discriminating phytoplankton pigment assemblages was evaluated by using an objective criterion of cluster similarity, the cophenetic index (Torrecilla et al., 2011). This index, which ranges from 0 to 1, measures how two cluster trees preserve their structure between data objects. In this study, it provided a measure of similarity between the optical-based cluster trees (i.e.  $a_{ph}(\lambda)$ - and  $R_{rs}(\lambda)$ -based partitions, respectively) and a reference cluster tree obtained from the HPLC pigment information. As discussed below, the cluster partition obtained from the pigment data served us as a reference for partitioning our data set into distinct groups, each characterized by a different phytoplankton pigment composition. To minimize variability in pigment composition associated with changes in phytoplankton biomass, the input to the cluster analysis in this case was represented by the ratio of individual pigment concentrations to the surface TChl-*a*. In addition, an Euclidean distance was utilized to generate the pigment-based cluster partition, instead of the angular distance used for the analysis of the spectral data. This type of distance pointed out differences in magnitude of ratios of concentrations of individual pigments to TChl-*a* rather than differences in shape.

Multivariate analyses were conducted with the statistical computing software “R” (R Development Core Team, 2008). Two matrices of similarity by station were created, one for the pigment composition and one for the environmental variables. As for the hierarchical cluster analysis, each station’s pigment concentrations were scaled relative to TChl-*a* to account for differences in magnitude and a similarity matrix was created using Euclidean distance. The environmental variables included for the analysis were surface temperature and salinity as well as location (latitude). As recommended by Clarke and Gorley (2001), environmental parameters were normalized to have a mean

**BGD**

8, 7165–7219, 2011

## Bio-optical provinces in the eastern Atlantic Ocean

B. B. Taylor et al.

Title Page

Abstract

Introduction

Conclusions

References

Tables

Figures

◀

▶

◀

▶

Back

Close

Full Screen / Esc

Printer-friendly Version

Interactive Discussion



---

**Bio-optical provinces  
in the eastern  
Atlantic Ocean**

---

B. B. Taylor et al.

---

[Title Page](#)[Abstract](#)[Introduction](#)[Conclusions](#)[References](#)[Tables](#)[Figures](#)[◀](#)[▶](#)[◀](#)[▶](#)[Back](#)[Close](#)[Full Screen / Esc](#)[Printer-friendly Version](#)[Interactive Discussion](#)

of zero and a standard deviation of 1 in order to account for differing units between variables and a similarity matrix between samples was also created using Euclidean distance. The full biological similarity matrix, based on pigment concentrations, was compared to similarity matrices of differing subsets of parameters as defined by Clarke and Ainsworth (1993) in order to identify those parameters best correlated. The first comparison was that of the more typical “BIO-ENV” setup whereas the fixed biological similarity matrix was correlated (Spearman rank) to an environmental similarity matrix with varying combinations of included parameters. The second comparison was between the fixed biological similarity matrix and a variable similarity matrix with differing subsets of included pigments, i.e. “BIO-BIO” (Clarke and Warwick, 1998, 2001; Clarke and Gorley, 2001). The BIO-BIO setup allowed for the identification of those pigments most responsible for the overall sample similarities. Due to the high search space of 23 pigments ( $2^{23} - 108,388,607$  possible subset combinations) a stepwise BIO-BIO procedure, “BVSTEP” (Clarke and Warwick, 1998), was used to efficiently search the subset space for the best combination up to a defined maximum correlation ( $\rho = 0.99$ ).

Ordinations of samples by non-metric multi-dimensional scaling (MDS) were plotted to help visualize sample similarities in terms of community pigment composition. Additional vectors were fit to the MDS ordination for the variables identified by the BIO-ENV and BIO-BIO routines above using the “envfit” function of the R package “vegan” (Oksanen et al., 2010).

Within clusters, differences in environmental parameters (TChl-*a*, surface temperature and salinity, depths of the deep chlorophyll maximum (DCM),  $Z_{eu}$  and  $Z_m$  (sigma)) were tested following an initial Shapiro-Wilk’s *W*-test of normality. Normally distributed data were tested with the independent t-test and non-normally distributed data were tested with a Mann-Whitney-U-test. All tests were considered significant when  $p < 0.05$ .

## 2.4 Satellite data

Mean values of marine phytoplankton Chl-*a* concentrations for November 2008 in selected areas around the ANT XXV-1 cruise were calculated within a 6' spatial grid resolution from the merged daily Full Product Set (FPS) of the GlobColour Archive (http://hermes.acri.fr/). The GlobColour Chl-*a* product is based on the merging of MERIS, SeaWiFS and MODIS level-2 data with the GSM model and algorithm, developed by Maritorena and Siegel (2005), over the whole globe with the best resolution of 4.6 km. These Chl-*a* data have undergone an extensive validation based on a validation protocol published in Maritorena et al. (2010).

## 3 Results

### 3.1 Physical and biological parameters at the sea surface

Sea-surface temperature and salinity data from the on-board thermosalinograph as well as Chl-*a* fluorescence data from the FRRF are depicted in Fig. 2. At the top of the graphic the locations and numbers of the discrete stations are depicted. Temperature and salinity values follow the trend that has been frequently reported (e.g. Sarthou et al., 2003). The Chl-*a* data show distinct features encountered during this cruise. These three data sets allowed us to identify some of the oceanographic features typical for the waters crossed by the ship's track. When exiting the English Channel (EC) the vessel crossed a tidal front (T), characterised by a drop in temperature at the eastern edge of the front and a peak in Chl-*a* fluorescence. The ship track then followed the eastern edge of the Northern Subtropical Gyre, the surface water temperature consistently increasing to a maximum of 30 °C at 7.6° N. At ~22° N and ~15° N the ship's track touched the edge two phytoplankton blooms (B1 and B2). Between ~12° N and ~2° N we encountered the Tropical Salinity Minimum Zone (TSM) associated with the heavy precipitation typical for this area, with a salinity minimum of 33.8 at 4.8° N. The

**BGD**

8, 7165–7219, 2011

## Bio-optical provinces in the eastern Atlantic Ocean

B. B. Taylor et al.

Title Page

Abstract

Introduction

Conclusions

References

Tables

Figures

◀

▶

◀

▶

Back

Close

Full Screen / Esc

Printer-friendly Version

Interactive Discussion



TSM Zone was followed by the Equatorial Upwelling (EqU) characterised by lower temperatures and higher salinity as well as a peak in Chl-*a* fluorescence. A steeper decrease in temperature and increase in salinity gives an indication that we crossed the Angola/Benguela front (AF) at  $\sim 12^\circ$  S. The Benguela current marks the north-eastern boundary of the Southern Subtropical Gyre and the last section of the expedition followed this boundary towards Cape Town, South Africa.

### 3.2 Phytoplankton composition

Figure 3 illustrates the results of the two methods employed to interpret the pigment data of surface samples only are shown in. The size classes method gives a comprehensible result with some clear features (Fig. 3a). The microplankton shows three distinct peaks at the stations in the English Channel (EC) and in the blooms (B1 and B2). Picoplankton dominates the community in the tropical and subtropical oligotrophic waters as has been reported before (Zubkov et al., 1998, 2000; Gibb et al., 2000; Heywood et al., 2006; Tarran et al., 2006; Aiken et al., 2009) whereas nanoplankton and picoplankton are relatively evenly distributed in all other areas of the transect.

Figure 3b shows the results of the CHEMTAX analysis. The colours have been chosen to match Fig. 3a, i.e. phytoplankton groups have been assigned to the respective size classes. Diatoms and dinoflagellates contribute to the microplankton, the cryptophytes, green algae (including chlorophytes and prasinophytes), pelagophytes and haptophytes have been assigned to the nanoplankton and the cyanobacteria are picoplankton. We are aware that this is only a very crude classification as most groups contribute to more than one size class. In this classification we lack the pico-eukaryotes, which also play an important role in the oligotrophic waters (Aiken et al., 2009). However, for an overview of the phytoplankton community, this approach is a helpful tool for the interpretation of pigment data.

Both approaches generalise from pigment composition either directly onto size classes or in the case of the CHEMTAX method from pigment ratios to phytoplankton groups, which have been consecutively grouped into size classes. Although different

Title Page

Abstract

Introduction

Conclusions

References

Tables

Figures



Back

Close

Full Screen / Esc

Printer-friendly Version

Interactive Discussion



calculations stand behind the results, the outcome of both methods is quite similar. The microplankton is generally lower in the CHEMTAX calculation, which gives slightly higher values to the groups attributed to the nanoplankton, but the general trend is reproduced with both methods. The fact that microplankton is probably overestimated in the size classes is imminent to the approach as Fuco is completely attributed to the microplankton whereas the CHEMTAX method accounts for the fact that Fuco is also a precursor for 19HF and 19BT and is therefore also partially attributed to the nanoplankton.

Flow cytometric and microscopic data were not available for all stations. The results will be used for clarification of specific stations or clusters in the discussion, but will not be shown here in detail.

### 3.3 Cluster analysis and multivariate statistics

The cluster analysis based on the pigment data resulted in six major clusters (Fig. 4). Each of the six clusters has been assigned a roman number and a different symbol, which will be also reproduced in the other cluster trees based on hyperspectral information. A clear north-to-south structure could be distinguished when stations corresponding to each cluster were plotted on a map (Fig. 1). Due to different pigment composition, stations 11, 12, 13, 19, 20 and 38 clustered away from their geographical neighbours (“outliers”). The clusters and “outliers” will be described in further detail below.

The BIO-ENV and BIO-BIO identified the pigments and environmental factors which best correlate with the sample similarities (Fig. 5, Tables 3 and 4). Figure 5 shows the stations plotted according to the MDS analysis, which clearly separated the clusters identified by HCA. Vectors show the directions of maximum correlation between the samples and associated variables. The analysis of the environmental variables (surface temperature, salinity and latitude) revealed the combination of latitude and temperature to be best correlated with pigment similarities ( $\rho = 0.27$ ; Fig. 5a). In terms of pigments the analysis between the full matrix with 23 pigments and varying subsets

## Bio-optical provinces in the eastern Atlantic Ocean

B. B. Taylor et al.

Title Page

Abstract

Introduction

Conclusions

References

Tables

Figures



Back

Close

Full Screen / Esc

Printer-friendly Version

Interactive Discussion



of this pigment matrix identified the combination of *DVa*, *Zea*, *Fuco*, *DVb*, and *Chl-a* to be mainly responsible for the calculated similarities between samples ( $\rho = 0.98$ ; Fig. 5b).

The cluster analysis was also performed based on  $a_{ph}(\lambda)$ -spectra for all 48 stations.

Figure 6 depicts the corresponding hierarchical cluster tree and the symbols of the pigment-based clustering for each station. The partition provided by the cluster analysis based on the  $a_{ph}(\lambda)$ -data is quite similar to the partition obtained using pigment information, which is reflected in the large value of the cophenetic index of 0.703 (Table 5). In order to optimize our performance, a sensitivity test of the cluster analysis regarding the choice of the spectral range was necessary (see also Torrecilla et al., 2011a). In accordance with other studies, the best degree of similarity between these two cluster trees (i.e. the highest cophenetic index) was obtained when the  $a_{ph}(\lambda)$ -spectrum was analyzed over the spectral range from 435 to 520 nm, where the most relevant pigments show their main absorption characteristics. Considering this optimal spectral range, cluster I, II, V and VI were exactly reproduced by the  $a_{ph}(\lambda)$ -data, clusters III and IV showed a few differences. In particular, stations 6 and 8 (which belong to cluster IV in the pigment-tree) classify with cluster III in the  $a_{ph}(\lambda)$ -tree. This may be attributable to a difference in the spectral shape of the  $a_{ph}(\lambda)$ -spectra of these two stations at around 470 nm (see Fig. S1 of the Supplement). The “outliers” of the pigment-based cluster tree 11, 12, 13 and 38 group with the cluster IV stations in the  $a_{ph}(\lambda)$ -tree. The main difference which singles them out in the pigment-tree is the presence of a considerable amount of *DVb*, which has its main absorption peak at 479 nm (see Fig. S2 of the Supplement). *Zea* and 19HF – which are the dominant pigments in cluster IV – also absorb strongly at that wavelength, which may explain why the  $a_{ph}(\lambda)$ -spectra are similar even if the pigment composition differs. Stations 19 and 20 were also considered “outliers” in the pigment-tree due to the dominance of *Fuco* in the samples. These stations were located just on the outer rim of a diatom bloom off the coast of Western Sahara and Mauritania (see below) which also characterized station 21. Station 21 clusters with station 24 and 25 in the pigment-tree as it was dominated

**Bio-optical provinces  
in the eastern  
Atlantic Ocean**

B. B. Taylor et al.

Title Page

Abstract

Introduction

Conclusions

References

Tables

Figures

◀

▶

◀

▶

Back

Close

Full Screen / Esc

Printer-friendly Version

Interactive Discussion



by Fuco, but stations 19 and 20 had a smaller percentage of Fuco (compared to total pigment) and were also characterized by the presence of *DVa* which delineated the stations before and after the bloom. Due to such differences in pigment composition it could be expected that these stations also partition separately with the absorption spectra. However, only station 19 clustered alone in the  $a_{ph}(\lambda)$ -tree; station 20 was associated with the cluster IV stations.

To explore the potential of remote sensing information in distinguishing different bio-optical provinces, the partition of the stations was also carried out based on 22  $R_{rs}(\lambda)$ -spectra (Fig. 7). This cluster analysis also yielded satisfactory results with a cophenetic index of 0.624 (Table 5). As reported in past studies (Torrecilla et al., 2011b), a good performance was only achieved when considering the second derivative of  $R_{rs}(\lambda)$ -spectra over the spectral range of 435 to 580 nm. Our ability to discriminate phytoplankton pigment assemblages from the derivative of  $R_{rs}(\lambda)$ -spectra was optimized by selecting the most suitable parameters used in the spectral derivative computations. In particular, we determined that the optimal values for the smoothing filter window and band separation were 9 nm for remote-sensing reflectance. Due to time constraints at the start of the cruise, no  $R_{rs}(\lambda)$  measurements were collected at the stations corresponding to clusters I and II. Whereas clusters III, V and VI were well reproduced, cluster IV showed some discrepancies, similar to the analysis based on  $a_{ph}(\lambda)$ -data. The same outlier stations 12, 20 and 38 which clustered separately in the pigment-based tree due to the high concentration of *DVb*, were associated with the cluster IV stations in the optical data (see Fig. S3 of the Supplement). Station 6 (cluster IV in the pigment-tree) was singled out in the  $R_{rs}(\lambda)$ -tree.

## Cluster characterization

Table 6 summarizes the main characteristics of the pigment-based clusters which are discussed in further detail below.

Cluster I comprised only station 1, which was located in the English Channel. It was clearly different from all other stations. The pigment composition was dominated

**BGD**

8, 7165–7219, 2011

## Bio-optical provinces in the eastern Atlantic Ocean

B. B. Taylor et al.

Title Page

Abstract

Introduction

Conclusions

References

Tables

Figures

◀

▶

◀

▶

Back

Close

Full Screen / Esc

Printer-friendly Version

Interactive Discussion



by Chl-*a*, Fuco and Chl-*b*, the CHEMTAX interpretation suggested that diatoms and green algae were the main contributors to the phytoplankton assemblage. Pigment composition and flow cytometry data confirmed that prochlorophytes were absent at this station as could be expected from a coastal area and temperate latitudes. The clustering of the absorption data also separated this station from the rest.

Cluster II was again composed of a single station (station 2) with a unique pigment signature. The local phytoplankton bloom and the strong stratification of this station observed in the temperature and density profiles suggested that we crossed a tidal front. Figure 8 shows a satellite image of surface Chl-*a* with the in-situ data plotted as coloured circles. Pigment, microscopic and flow cytometric analysis imply that the bloom was mainly composed of haptophytes, green algae, dinoflagellates and phycobilin-containing cyanobacteria (*Synechococcus*). The pigments that made this station unique in terms of pigment data were a high concentration of Peri (up to 100 times more concentrated than at any other station) and the lack of DV*a*. The cluster analysis of absorption spectra also singled this station out.

Cluster III was geographically rather patchy, although 3 of the 5 stations that made out the cluster (Stations 3–5) were located to the South of Cluster II, west of the Bay of Biscay. The two other stations (station 7 and 22) are geographically scattered among clusters IV and V. The dominant pigments were Chl-*a* and 19HF and the main phytoplankton groups at these stations were haptophytes, green algae and pelagophytes. Absorption spectra of those stations did also not differ significantly.

Cluster IV was the biggest cluster and united all stations with DV*a*, Zea and 19HF as dominant pigments. As can be expected from this pigment composition the flow cytometry analysis revealed high cell number of prochlorophytes and a smaller number of phycoerythrin-containing cyanobacteria at most of the stations joined in this cluster. CHEMTAX calculations confirmed the dominance of *Prochlorococcus* (HL), followed by haptophytes, pelagophytes and *Synechochoccus*-type cyanobacteria. The size class calculation also corroborated a dominance of picophytoplankton with over 50% at most stations. The absorption spectra were very similar for these stations, so that – with the

**BGD**

8, 7165–7219, 2011

## Bio-optical provinces in the eastern Atlantic Ocean

B. B. Taylor et al.

Title Page

Abstract

Introduction

Conclusions

References

Tables

Figures

◀

▶

◀

▶

Back

Close

Full Screen / Esc

Printer-friendly Version

Interactive Discussion



exception of stations 6, 8, 19 and 20 – the clustering based on absorption data formed the same cluster.

Geographically however, these stations could be divided into a northern (IV-N, comprising stations 6, 8–10 and 14–18) and a southern sub-cluster (IV-S, stations 26–40, with the exception of station 38), which were separated by cluster V. The Chl-*a* concentrations and the oceanographic data also confirmed this division: thermoclines and pycnoclines were significantly deeper in the northern than in the southern sub-cluster ( $p < 0.01$ ). The DCM was not as clearly defined in the northern cluster as it was in the southern sub-cluster, where we found a pronounced Chl-*a* peak just below 50 m at all stations. Most stations of the northern sub-cluster showed two Chl-*a* maxima, the second one often just below  $Z_{eu}$ . The surface TChl-*a*, surface salinity and  $Z_m$  were significantly lower in IV-S than in its northern counterpart, whereas SST was significantly higher ( $p < 0.05$ ). The gradient between nutrient-poor waters at the surface and nutrient-rich waters at depth was much stronger in the southern compared to the northern sub-cluster ( $< 0.2 \mu\text{M}$  nitrate at the surface in both areas and  $5\text{--}10 \mu\text{M}$  nitrate at 200 m in IV-N compared to  $> 20 \mu\text{M}$  nitrate at 200 m in IV-S; Koch and Kattner, 2011).

Sub-cluster IV-N, at the eastern edge of the North Atlantic Subtropical Gyre along the Canary Current, bordered onto the south of station 5 (cluster III), but was also not consistent geographically. Several outliers and a station belonging to another cluster (station 7, Cluster III) were scattered among the stations of cluster IV-N. Sub-cluster IV-S was separated from IV-N by cluster V and was geographically a very consistent cluster. It extended from approximately  $12^\circ \text{N}$  to  $12\text{--}13^\circ \text{S}$ , encompassing the Equatorial Counter Current and the Southern Equatorial Current.

Cluster V comprised the “Bloom stations” with Fuco as the dominant diagnostic pigment and high TChl-*a* concentrations between  $1.3$  and  $5.3 \text{ mg m}^{-3}$ . The cruise track crossed two different blooms (Fig. 9) and stations 21, 24 and 25 lie at the edge of these blooms. Note that the satellite picture is a 4 week average, which may explain the difference between the in-situ measurements and the satellite data. At the point in time when we passed the bloom, it probably had slightly different dimensions than on the

**BGD**

8, 7165–7219, 2011

## Bio-optical provinces in the eastern Atlantic Ocean

B. B. Taylor et al.

Title Page

Abstract

Introduction

Conclusions

References

Tables

Figures

◀

▶

◀

▶

Back

Close

Full Screen / Esc

Printer-friendly Version

Interactive Discussion



averaged picture. The blooms mainly consisted of diatoms (approx. 60 % of TChl-*a*), some haptophytes and *Synechococcus*-type cyanobacteria. In the clustering of the  $a_{ph}(\lambda)$ -data station 21 was separated from station 24 and 25. The samples 19 and 20 (outliers) were taken on the edge of the first bloom. Their main diagnostic pigments were Fuco (characteristic for diatoms and for the bloom) and DVa (characteristic for *Prochlorococcus* and the open ocean).

The stations belonging to cluster VI were clearly defined and separated through their bio-optical traits from the other stations. Geographically they were also located together at the eastern edge of the Southern Subtropical Gyre, adjoining cluster IV-S to the south. The stations in this cluster were dominated by haptophytes (approximately 45 % of total biomass) and *Synechococcus*-type cyanobacteria. Dominant marker pigments were Zea and 19 HF, which influence strongly the shape of the absorption spectra (see Fig. S2 of the Supplement). The  $a_{ph}(\lambda)$ -spectra of the stations of cluster VI also formed one well separated cluster in the  $a_{ph}(\lambda)$ -tree. The microscopic analysis identified the haptophytes as coccolithophores.

## 4 Discussion

Our study showed a clustering of the different stations into different regional clusters on the basis of pigment composition,  $a_{ph}(\lambda)$ - and  $R_{rs}(\lambda)$ -spectra. In the following section we discuss the mechanisms which determine the phytoplankton community structure and the significance of the revealed bio-optical regions in comparison with another biogeography.

### 4.1 Mechanisms determining phytoplankton community structure

#### 4.1.1 Environmental factors

The multivariate analysis identified the combination of temperature and latitude as the main environmental variables responsible for the spread of the data on the basis of

**BGD**

8, 7165–7219, 2011

## Bio-optical provinces in the eastern Atlantic Ocean

B. B. Taylor et al.

Title Page

Abstract

Introduction

Conclusions

References

Tables

Figures

◀

▶

◀

▶

Back

Close

Full Screen / Esc

Printer-friendly Version

Interactive Discussion



pigment composition (Fig. 5b). Salinity did not improve the correlation (Table 3). In this analysis only temperature, salinity and latitude were incorporated as other possible environmental variables, such as  $Z_{eu}$ ,  $Z_m$  or nutrients, were only available for a smaller subset of stations.

5 Temperature was the most important environmental variable if only one variable was considered. It is an important variable in itself and the temperature dependence of phytoplankton has been frequently reported in the literature (e.g. Platt et al., 2005; Li, 2009; Burgmer and Hillebrand, 2011). The effect of temperature can be direct, as many species have a tolerance of a certain temperature range outside of which they  
10 cannot survive (e.g. Partensky et al., 1999; Breitbarth et al., 2007), or can be indirect by influencing predators, photosynthesis rates or nutrient availability (Carder et al., 1999; Sathyendranath et al., 2001; Bouman et al., 2003; Platt et al., 2005).

Temperature is a variable which is commonly recorded, easy to measure and can be observed from satellites, which is an important issue in the wake of global observations  
15 of ocean dynamics. Moreover, temperature is part of other physico-chemical processes such as stability of the water column (Platt et al., 2005) and thus can be seen as the manifestation of more complex physical structures. Bouman et al. (2003) were able to explain between 43 and 49% of the variance in the specific absorption coefficients of phytoplankton at certain wavelengths with temperature. They showed that temper-  
20 ature can be a proxy for two main turbulence-nutrient regimes: high temperatures are generally associated with conditions of low turbulence and low nutrients, low temperatures with those of high turbulence and high nutrients. Platt et al. (2005) identified a clear temperature dependence for phytoplankton community structure. Temperature has even been used to estimate concentrations of nitrate over regional and global  
25 scales (Sathyendranath et al., 1991; Switzer et al., 2003).

Including latitude improves the correlation and thus allows us to explain more of our data variability than with temperature alone. Latitude was used as an environmental factor as it implies several variables which were not available at all or not at the resolution needed for a statistical analysis. The transect covered several contrasting

---

**Bio-optical provinces  
in the eastern  
Atlantic Ocean**B. B. Taylor et al.

---

[Title Page](#)[Abstract](#)[Introduction](#)[Conclusions](#)[References](#)[Tables](#)[Figures](#)[Back](#)[Close](#)[Full Screen / Esc](#)[Printer-friendly Version](#)[Interactive Discussion](#)

physico-chemical regimes or climatic zones (gyres, upwelling, temperate, subtropical, tropical regions, coastal and open waters) and latitude could be the environmental factor standing for the influence of such complex variables as light availability, cloud cover, mixed or stratified waters, upwelling etc. However, the low Spearman rank correlation factor of 0.266 suggests that many more factors are involved in the complex dynamics behind the pigment/phytoplankton distribution and that latitude alone cannot cover the variability caused by other physical forces. The link between physical forcing and ecosystem structure has been established by Margalef (1978) more than three decades ago and has been corroborated and added on to by several authors (e.g. Agustí and Duarte, 1999; Cullen et al., 2002; Wang et al., 2009). Phytoplankton ecology is described as an expression of the turbulence and nutrient conditions presented by ocean physics, although it should be kept in mind that not all limiting nutrients are supplied from below through mixing and/or upwelling processes. Iron can be introduced through Aeolian deposits, as could be seen in the case of the second bloom encountered on our cruise, or nitrogen can be fixed from the atmosphere by diazotroph algae.

The analysis emphasizes that the forces behind phytoplankton community structure (here expressed through the index of pigment distribution) are complex and cannot easily be reduced to one variable. However, in combination with another biological or bio-optical variable such as TChl-*a*, phytoplankton absorption or pigment composition, temperature can be a powerful variable to supplement the measurements and identify boundaries of bio-optical provinces.

#### 4.1.2 Pigments

The BIO-BIO routine identified the combination of the five pigments DV*a*, Zea, Fuco, DV*b* and Chl-*a* to be mainly responsible for the calculated similarity “distances” between samples (Fig. 5b, Table 4). By including these five pigments the Spearman rank correlation coefficient  $\rho$  reached a value of 0.98. DV*a* alone already accounts for  $\rho = 0.73$ , which rises to  $\rho = 0.85$  when Zea is included. Fuco as a representative of

### Bio-optical provinces in the eastern Atlantic Ocean

B. B. Taylor et al.

Title Page

Abstract

Introduction

Conclusions

References

Tables

Figures

◀

▶

◀

▶

Back

Close

Full Screen / Esc

Printer-friendly Version

Interactive Discussion



larger-celled groups such as diatoms, haptophytes or pelagophytes (in the latter two groups it is present as a precursor for the marker pigments 19HF and 19BT, respectively) is the third important predictor, followed by *DVb*. With *DVb*, *DVa* and *Zea* three markers specific for cyanobacteria are identified as important pigments correlated to the distribution of phytoplankton groups. Figure 5b demonstrates that these three pigments dominate the formation of cluster IV and of the outliers 11, 12, 13 and 38, which are conspicuous due to their high concentration of *DVb*. *Chl-a*, which occurs in all phytoplankton groups other than *Prochlorococcus* is the fifth main variable correlated to the pigment distribution of our samples and spreads the samples in the opposite direction than *DVa*.

*DVa* and *DVb* are unique marker pigments for *Prochlorococcus* and do not occur in other species (Chisholm et al., 1992; Goericke and Repeta, 1992). The fact that they are two of the main predictors of the clustering of the pigment matrix emphasizes the importance of this group of cyanobacteria. *Prochlorococcus*, one of the three known genera of the prochlorophytes, was discovered in the late 1980's (Chisholm et al., 1988) and is – with an approximate mean cell size of 0.6  $\mu\text{m}$  – the smallest known photosynthetic organism (Partensky et al., 1999). It has been estimated to account for 30–60% of the TChl-*a* in subtropical oligotrophic regions and thus plays a key role in global primary production and carbon cycling (Partensky et al., 1999; Partensky and Garczarek, 2010). *Prochlorococcus* occurs ubiquitously between 40° N and 40° S throughout the euphotic zone and even below. Genetic and physiological diversity make it unique and explain the numerical abundance and broad habitat. Recently developed molecular approaches have revealed different ecotypes which dominate at different depths or latitudes (West and Scanlan, 1999; Zinser et al., 2007; Zwirgmaier et al., 2007). Generally two main groups of ecotypes of *Prochlorococcus* have been distinguished: high-light adapted (HL) and low-light adapted (LL) types. Pigment analysis can differentiate between these two ecotype groups as they differ in their *DVb*:*DVa* ratio (Moore and Chisholm, 1999; Veldhuis and Kraay, 2004). *DVb* is specific for LL ecotypes of *Prochlorococcus* as it absorbs the blue light that penetrates deepest into

**BGD**

8, 7165–7219, 2011

## Bio-optical provinces in the eastern Atlantic Ocean

B. B. Taylor et al.

Title Page

Abstract

Introduction

Conclusions

References

Tables

Figures

◀

▶

◀

▶

Back

Close

Full Screen / Esc

Printer-friendly Version

Interactive Discussion



the water column (Moore and Chisholm, 1999), and explains the spread of the samples 11, 12, 13 and 38 which are different from all other samples due to the high concentration of *DVb*. The diversity of the LL group is much wider than that of HL group (Partensky and Garczarek, 2010). Some LL ecotypes have been found to co-occur with HL ecotypes at the surface, especially in mixed water columns at higher latitudes (Zwirgmaier et al., 2007) and thus could be a proxy for mixed rather than stratified conditions. Johnson et al. (2006) showed that temperature is significantly correlated with shifts in *Prochlorococcus* ecotype abundance, thus linking our main biological with the major environmental predictor. Temperature explains the spread of the data on the MDS plots in the same direction as *DVa*.

*Zea* is a general marker for all cyanobacteria and occurs in both main genera *Synechococcus* and *Prochlorococcus*. Between *DVa* and *Zea* most of cluster IV – which is dominated by small cells – is explained. Fuco is a marker pigment for diatoms, but is also – as pointed out earlier – a precursor for 19HF and 19BT which are specific for haptophytes and pelagophytes (Vesk and Jeffrey, 1987; Wright and Jeffrey, 1987). Clusters I, II, III and V, dominated by nanoplankton and/or microplankton, are mainly described by Fuco and Chl-*a*.

Here, we show that a few pigments with distinct optical features can describe a clustering based on the matrix of a broad pigment composition of each sample. It became clear, that the picophytoplankton and more specifically *Prochlorococcus* are responsible for most of the variability in the eastern Atlantic Ocean. Dandonneau and Niang (2007) also observed that differences in pigment composition in their samples from the North Atlantic and Tropical Pacific could mainly be explained by their *DVa* content. Thus we agree with Marañón et al. (2001) that picophytoplankton should not be regarded as a background and relatively invariant component of the community, but rather as a main driver of most of the latitudinal variability in total photoautotrophic biomass and production in the tropical and subtropical East Atlantic.

**BGD**

8, 7165–7219, 2011

## Bio-optical provinces in the eastern Atlantic Ocean

B. B. Taylor et al.

Title Page

Abstract

Introduction

Conclusions

References

Tables

Figures

◀

▶

◀

▶

Back

Close

Full Screen / Esc

Printer-friendly Version

Interactive Discussion



## 4.2 Bio-optical geography

By applying an unsupervised hierarchical cluster analysis to pigment and hyperspectral data from the eastern Atlantic Ocean, we have demonstrated the potential applicability of pigment composition, absorption coefficients and remote sensing reflectance for identifying different bio-optical units or provinces. To assess our bio-optical approach with an established biogeography, we compare our provinces/clusters to the widely used system defined by Longhurst (2007). Longhurst proposes a global partitioning into 4 biomes or basic vegetation types within the pelagic realm of the oceans: the Polar, Westerlies, Trades and Coastal biome. Within the biomes, 51 provinces are defined on the basis of a global dataset including satellite images of surface chlorophyll fields and regional oceanography data, also considering many previous proposals for partitioning the oceans. Although the boundaries of the provinces are forced into a static grid as a matter of convenience, Longhurst points out that the position of the borders is dynamic and varies on annual, seasonal or even shorter time scales. As our optical data are not continuous, we occasionally include the continuous temperature, salinity and Chl-*a* measurements to identify the boundaries. In Fig. 1 the stations with their assigned cluster symbols are plotted on a map depicting Longhurst provinces (shapefile from VLIZ, 2009).

Cluster I and II belong to the continental shelf of Western Europe, described by Longhurst as the Northeast Atlantic Shelves Province (NECS). The English Channel is strongly dominated by tidal forces, a fact that is corroborated by the density, temperature and Chl-*a* fluorescence profiles of these stations which show strong mixing of the water column. Our analysis separates the two stations into two clusters which is probably due to the fact that station 2 (cluster II) was situated in a tidal front. The boundary to the next cluster at this point in time, was probably situated just after station 2, at around 47.5° N where a sudden rise in sea surface temperature and salinity occurs after the tidal front (Figs. 2 and 8).

**BGD**

8, 7165–7219, 2011

### Bio-optical provinces in the eastern Atlantic Ocean

B. B. Taylor et al.

Title Page

Abstract

Introduction

Conclusions

References

Tables

Figures

◀

▶

◀

▶

Back

Close

Full Screen / Esc

Printer-friendly Version

Interactive Discussion



The stations joined in cluster III do not all belong to the same geographical province. Stations 3–5 lie in the south-east corner of Longhurst's North Atlantic Drift province (NADR). In this province wind speed in autumn and winter is greater than anywhere else except in the Southern Ocean which induces anomalous deepening of the mixed layer to more than 500 m along the European continental edge. Stations 3 and 5 show a pycnocline at ~100 m depth during our cruise at the beginning of November which might deepen as winter progresses. Stations 3–5 also show no DCM. For stations 7 and 22 we do unfortunately not have CTD profiles for comparison, but we can deduce some information from the data of station 6. Especially the Chl-*a* fluorescence profile data shows a change from station 6 southwards where a small DCM could be detected and after station 5 pycno- and thermocline move upwards. Bio-optical traits join these stations together, but oceanographic data and geography show that stations 7 and 22 belong to different oceanic provinces.

The sub-cluster IV-N lies within Longhurst's North Atlantic Subtropical Gyral Province (East) (NAST(E)). However, this area is bio-optically not consistent and many outliers lie alongside the stations of cluster IV-N. These inconsistencies might be explained by typical physical processes in this region such as eddy-driven vertical advection, internal waves or salt fingering (McGillicuddy et al., 2003; Oschlies et al., 2003; Dietze et al., 2004; Dandonneau and Niang, 2007). Particularly the occurrence of DV*b* in the outliers 11–13 suggest a recent upwelling of LL *Prochlorococcus* ecotypes or a mixed water column (see above). Moreover this region is influenced by Mediterranean Water eddies (meddies), which flow out of the Strait of Gibraltar and move southwards once they have detached from the continental slope. Although meddies are usually encountered at several 100 m depth they have been shown to influence surface water characteristics (Richardson et al., 2000; Siedler et al., 2005). Another possible disturbance comes from seamounts, which can also spawn eddies and have influence on the water column above them (Comeau et al., 1995; Christiansen and Wolff, 2009). Station 12 (outlier) for example lies exactly above the Seine seamount at 24° N and 14° W.

**BGD**

8, 7165–7219, 2011

## Bio-optical provinces in the eastern Atlantic Ocean

B. B. Taylor et al.

Title Page

Abstract

Introduction

Conclusions

References

Tables

Figures

◀

▶

◀

▶

Back

Close

Full Screen / Esc

Printer-friendly Version

Interactive Discussion



The sub-cluster IV-S with stations 26–40 is also geographically a very consistent cluster and lies within Longhurst's Eastern Tropical Atlantic Province (ETRA). It extends from approximately 12° N to 12–13° S, encompassing the Equatorial Counter Current and the Southern Equatorial Current. The boundaries are clearly defined to the north by the bloom (cluster V discussed below) and to the south by the Angola Frontal System (between 12 and 13° S) characterized by a change in PFTs and an abrupt increase in salinity. To the north of the Equator, we encountered the typical Tropical Salinity Minimum Zone, followed by the Equatorial Upwelling identified by a rise in salinity, a drop in temperature and higher Chl-*a* concentrations (see Fig. 2). Perez et al. (2005) describe the typical phytoplankton community or size structure for this region as rather constant with the contribution of picoplankton to total Chl-*a* always exceeding 45 %, a description which is corroborated by our results.

Although the pigment composition joins the “bloom-stations” together (cluster V), it is clear from our continuous Chl-*a* measurements and the satellite picture that the station belong to two different blooms (Figs. 2 and 9). In the clustering of the  $a_{ph}(\lambda)$ -data station 21 is also separated from station 24 and 25. The northern bloom (station 21) is due to a major upwelling focus in this area south of Cape Blanc (Western Sahara) off the coast of Mauretania. The outliers 19 and 20 are samples that were taken on the edge of the bloom and represent a transition zone between the oligotrophic waters of the tropical Atlantic and the upwelling area. Their main diagnostic pigments were Fuco (characteristic for diatoms and for the bloom) and DVa (characteristic for *Prochlorococcus* and oligotrophic areas). There are no profile data from station 21, but station 20 shows a very strong DCM at around 90 m with high TChl-*a* concentrations (1.6 mg m<sup>-3</sup>) with the same dominant pigments as the surface bloom.

The southern bloom (stations 24 and 25) lies within the African dust veil where a special characteristic of the wind regime is the dust-laden nature of the northeast trades, wherever their back trajectory lies over the Saharan desert. These so-called Harmattan winds carry mineral dust over the ocean from 25° N to 10° S (Croot et al., 2004; Baker et al., 2006; Pohl et al., 2011). The  $a_{ph}(\lambda)$ -spectra of these two stations have

**BGD**

8, 7165–7219, 2011

## Bio-optical provinces in the eastern Atlantic Ocean

B. B. Taylor et al.

Title Page

Abstract

Introduction

Conclusions

References

Tables

Figures

◀

▶

◀

▶

Back

Close

Full Screen / Esc

Printer-friendly Version

Interactive Discussion



## Bio-optical provinces in the eastern Atlantic Ocean

B. B. Taylor et al.

Title Page

Abstract

Introduction

Conclusions

References

Tables

Figures

◀

▶

◀

▶

Back

Close

Full Screen / Esc

Printer-friendly Version

Interactive Discussion



very different shapes compared to all other samples of this cruise. The high absorption in the spectral region below 400 nm is very unusual and was present in all replicates of these stations. The most probable explanation for the altered spectral shape is dust retained on the filters resulting from the Aeolian dust deposits to the ocean. The results from aerosol and iron measurements from the same cruise show high concentrations of both at the relevant latitudes and thus confirm our hypothesis (Neogi et al., 2011 and P. Schmitt-Kopplin, personal communication, 2011).

Station 25 also shows a strong DCM with high TChl-*a* concentrations ( $2.2 \text{ mg m}^{-3}$ ). The DCM here however is much shallower (40 m) and consists of a different phytoplankton assemblage with 19 HF as the dominant marker pigment (haptophytes). Thus the bloom at the surface triggered through Aeolian deposits could be partially or fully unconnected to the phytoplankton community at depth. In Longhurst's biogeography both blooms would probably be assigned to the Canary Current Coastal Province (CNRV) which comprises the southerly coastal flow of the eastern boundary current of the North Atlantic from Cape Finisterre in North Portugal to Cape Verde in Senegal. The seaward boundary is defined by Longhurst to be approximately 200–400 km offshore and the cruise track was between 300 and 450 km offshore at these latitudes.

Geographically stations 22 and 23 lie in the same region and could theoretically also belong to CNRV although they have been clustered differently on the account of their pigment composition (cluster III and IV, respectively). These two stations lie between the two blooms and have comparatively low TChl-*a* concentrations ( $>0.5 \text{ mg m}^{-3}$ ). As the cruise track lies on the approximate boundary between CNRV and its western neighbour, the North Atlantic Tropical Gyral Province (NATV), these two station could also belong to NATV, which is characterized by the lowest TChl-*a* in the North Atlantic.

The stations belonging to cluster VI are clearly defined and separated through their bio-optical traits from the other stations. They differ in pigment composition,  $a_{\text{ph}}(\lambda)$ - and  $R_{\text{rs}}(\lambda)$ -spectra and are clearly located in Longhurst's South Atlantic Gyral Province (SATV), which comprises the anticyclonic circulation of the South Atlantic, excluding the coastal boundary currents. According to Marañón et al. (2000) we can expect

minimal Chl-*a* values in the central regions of the gyre and higher values around the periphery. This cruise sampled the eastern edge of the Southern Subtropical Gyre and yielded surface TChl-*a* values of  $0.32 \pm 0.09 \text{ mg m}^{-3}$ , which is approximately the same as in the respective area in the Northern Hemisphere (cluster IV-N, see Table 6).

5 The DCM at 30–50 m was not as sharp as in other areas and had about twice the amount of TChl-*a* than the surface, but very similar pigment composition. However, this does not necessarily mean that the DCM was also the biomass maximum, as it has been shown that the carbon to Chl-*a* ratio can decrease with depth in gyral areas (Marañón et al., 2000). The northern boundary of this province is clearly defined by  
10 our bio-optical data between station 40 and 41, around 12–13° N. This coincides fairly well with the boundary set by Longhurst for SATL (approximately 10° S). The Angola-Benguela-Front marks this boundary. It corresponds to the convergence zone between the north-moving surface waters of the Benguela and the south-flowing Angola Current, and could be identified with surface temperature and salinity data at exactly the position  
15 between the stations which mark the bio-optical boundary. The southern boundary is probably after our last discrete water sample at ~25° S when we entered the Benguela current.

## 5 Conclusions

Picophytoplankton, and among them specifically the genus *Prochlorococcus*, are responsible for most of the variability of PFTs in the eastern Atlantic Ocean. Our bio-optical clusters agree well with the established provinces established by Longhurst and thus can be used to classify areas of similar biogeography. However, in areas with high variability, such as along the Canary Current (cluster IV-N and most outliers) or at the NW African upwelling (cluster V) the Longhurst provinces do not harbour consistent  
20 phytoplankton assemblages. In such areas it would be advantageous to use a more flexible and dynamic approach to describe the ecosystem. Since pigment composition corresponded well with the remotely observable  $a_{\text{ph}}(\lambda)$ - and  $R_{\text{rs}}(\lambda)$ -spectra, this method  
25

### Bio-optical provinces in the eastern Atlantic Ocean

B. B. Taylor et al.

Title Page

Abstract

Introduction

Conclusions

References

Tables

Figures

◀

▶

◀

▶

Back

Close

Full Screen / Esc

Printer-friendly Version

Interactive Discussion



has potential to become an automated approach for the future. Hyperspectral sensors mounted on platforms such as buoys, gliders or satellites could provide the data to identify shifting boundaries of established provinces or to track exceptions from the rule in order to improve our understanding of the biogeochemical cycles in the ocean.

In terms of globally significant issues such as carbon export and primary production our optical approach represents a possibility for a fast and detailed assessment of the state of a temporally and spatially variable environment.

**Supplementary material related to this article is available online at:**

**<http://www.biogeosciences-discuss.net/8/7165/2011/>**

**[bgd-8-7165-2011-supplement.pdf](#)**.

*Acknowledgements.* We thank AWI, Helmholtz Impulse Fond, UTM-CSIC and OCEANET for funding. Part of this study was performed during a visit of Elena Torrecilla at the PHYTOOPTICS group supported by the Spanish National Research Council CSIC (project ANERIS PIF08-015) and the Spanish Ministry of Education (Ph.D. European Mentoring Program). We are grateful to NASA and ESA, particularly to the GlobColour project, for processing and supplying Satellite total Chl-*a* concentrations. We thank Erika Allhusen, Charlotte Klein, Mirko Lunau, Eva-Maria Nöthig and Sonja Wiegmann for help with the work on the field samples, Mariana Soppa and Gerd Rohardt for further data analysis. We thank the crew, principal investigators and other scientists on board the R/V *Polarstern* cruise ANTXXV-1 for support on board and fruitful discussions afterwards.

## References

- Agustí, S. and Duarte, C. M.: Phytoplankton chlorophyll *a* distribution and water column stability in the central Atlantic Ocean, *Oceanol. Acta*, 22, 193–203, 1999.
- Aiken, J., Pradhan, Y., Barlow, R., Lavender, S., Poulton, A., Holligan, P., and Hardman-Mountford, N.: Phytoplankton pigments and functional types in the Atlantic Ocean: A decadal assessment, 1995–2005, *Deep-Sea Res. Pt. II*, 56, 899–917, doi:10.1016/j.dsr2.2008.09.017, 2009.

## Bio-optical provinces in the eastern Atlantic Ocean

B. B. Taylor et al.

Title Page

Abstract

Introduction

Conclusions

References

Tables

Figures

◀

▶

◀

▶

Back

Close

Full Screen / Esc

Printer-friendly Version

Interactive Discussion



---

## Bio-optical provinces in the eastern Atlantic Ocean

---

B. B. Taylor et al.

[Title Page](#)
[Abstract](#)
[Introduction](#)
[Conclusions](#)
[References](#)
[Tables](#)
[Figures](#)
[Back](#)
[Close](#)
[Full Screen / Esc](#)
[Printer-friendly Version](#)
[Interactive Discussion](#)


- Baker, A. R., Jickells, T. D., Biswas, K. F., Weston, K., and French, M.: Nutrients in atmospheric aerosol particles along the Atlantic Meridional Transect, *Deep-Sea Res. Pt. II*, 53, 1706–1719, doi:10.1016/j.dsr2.2006.05.012, 2006.
- Barlow, R., Stuart, V., Lutz, V., Sessions, H., Sathyendranath, S., Platt, T., Kyewalyanga, M., Clementson, L., Fukasawa, M., Watanabe, S., and Devre, E.: Seasonal pigment patterns of surface phytoplankton in the subtropical southern hemisphere, *Deep-Sea Res. Pt. I*, 54, 1687–1703, doi:10.1016/j.dsr.2007.06.010, 2007.
- Barlow, R. G., Aiken, J., Holligan, P. M., Cummings, D. G., Maritorena, S., and Hooker, S.: Phytoplankton pigment and absorption characteristics along meridional transects in the Atlantic Ocean, *Deep-Sea Res. Pt. I*, 49, 637–660, 2002.
- Bouman, H. A., Platt, T., Sathyendranath, S., Li, W. K. W., Stuart, V., Fuentes-Yaco, C., Maass, H., Horne, E. P. W., Ulloa, O., Lutz, V., and Kyewalyanga, M.: Temperature as indicator of optical properties and community structure of marine phytoplankton: implications for remote sensing, *Mar. Ecol.-Prog. Ser.*, 258, 19–30, 2003.
- Breitbarth, E., Oschlies, A., and LaRoche, J.: Physiological constraints on the global distribution of *Trichodesmium* – effect of temperature on diazotrophy, *Biogeosciences*, 4, 53–61, doi:10.5194/bg-4-53-2007, 2007.
- Bricaud, A., Claustre, H., Ras, J., and Oubelkheir, K.: Natural variability of phytoplanktonic absorption in oceanic waters: Influence of the size structure of algal populations, *J. Geophys. Res.-Oceans*, 109, C11010, doi:10.1029/2004jc002419, 2004.
- Burgmer, T. and Hillebrand, H.: Temperature mean and variance alter phytoplankton biomass and biodiversity in a long-term microcosm experiment, *Oikos*, 120, 922–933, doi:10.1111/j.1600-0706.2010.19301.x, 2011.
- Carder, K. L., Chen, F. R., Lee, Z. P., Hawes, S. K., and Kamykowski, D.: Semianalytic Moderate-Resolution Imaging Spectrometer algorithms for chlorophyll a and absorption with bio-optical domains based on nitrate-depletion temperatures, *J. Geophys. Res.-Oceans*, 104, 5403–5421, 1999.
- Carr, M. E., Friedrichs, M. A. M., Schmeltz, M., Aita, M. N., Antoine, D., Arrigo, K. R., Asanuma, I., Aumont, O., Barber, R., Behrenfeld, M., Bidigare, R., Buitenhuis, E. T., Campbell, J., Ciotti, A., Dierssen, H., Dowell, M., Dunne, J., Esaias, W., Gentili, B., Gregg, W., Groom, S., Hoepffner, N., Ishizaka, J., Kameda, T., Le Quere, C., Lohrenz, S., Marra, J., Melin, F., Moore, K., Morel, A., Reddy, T. E., Ryan, J., Scardi, M., Smyth, T., Turpie, K., Tilstone, G., Waters, K., and Yamanaka, Y.: A comparison of global estimates of marine primary production from

## Bio-optical provinces in the eastern Atlantic Ocean

B. B. Taylor et al.

Title Page

Abstract

Introduction

Conclusions

References

Tables

Figures

◀

▶

◀

▶

Back

Close

Full Screen / Esc

Printer-friendly Version

Interactive Discussion



- ocean color, *Deep-Sea Res. Pt. II*, 53, 741–770, doi:10.1016/j.dsr2.2006.01.028, 2006.
- Chisholm, S. W., Olson, R. J., Zettler, E. R., Goericke, R., Waterbury, J. B., and Welschmeyer, N. A.: A novel free-living prochlorophyte abundant in the oceanic euphotic zone, *Nature*, 334, 340–343, 1988.
- 5 Chisholm, S. W., Frankel, S. L., Goericke, R., Olson, R. J., Palenik, B., Waterbury, J. B., Westjohnsrud, L., and Zettler, E. R.: *Prochlorococcus marinus* nov. gen. nov. sp.: an oxyphototrophic marine prokaryote containing divinyl chlorophyll *a* and chlorophyll *b*, *Arch. Microbiol.*, 157, 297–300, 1992.
- Christiansen, B. and Wolff, G.: The oceanography, biogeochemistry and ecology of two NE-Atlantic seamounts: The OASIS project, *Deep-Sea Res. Pt. II*, 56, 2579–2581, 2009.
- 10 Clarke, K. R. and Ainsworth, M.: A method of linking multivariate community structure to environmental variables, *Mar. Ecol.-Prog. Ser.*, 92, 205–219, 1993.
- Clarke, K. R. and Gorley, R. N.: *PRIMER v5: User Manual/Tutorial*, PRIMER-E Ltd., Plymouth, UK, 2001.
- 15 Clarke, K. R. and Warwick, R. M.: Quantifying structural redundancy in ecological communities, *Oecologia*, 113, 278–289, 1998.
- Clarke, K. R. and Warwick, R. M.: *Changes in Marine Communities: An Approach to Statistical Analysis and Interpretation*, 2nd edn., PRIMER-E Ltd, Plymouth, UK, 2001.
- Comeau, L. A., Vezina, A. F., Bourgeois, M., and Juniper, S. K.: Relationship between phytoplankton production and the physical structure of the water column near Cobb Seamount, Northeast Pacific, *Deep-Sea Res. Pt. I*, 42, 993–1005, 1995.
- 20 Croot, P. L., Streu, P., and Baker, A. R.: Short residence time for iron in surface seawater impacted by atmospheric dry deposition from Saharan dust events, *Geophys. Res. Lett.*, 31, L23s08 doi:10.1029/2004gl020153, 2004.
- 25 Cullen, J. J., Franks, P. J. S., Karl, D. M., and Longhurst, A.: Physical influences on marine ecosystem dynamics, in: *The Sea – Ideas and Observations on Progress in the Study of the Seas*, edited by: Robinson, A. R., McCarthy, J. J., and Rothschild, B. J., Harvard University Press, 2002.
- Dandonneau, Y. and Niang, A.: Assemblages of phytoplankton pigments along a shipping line through the North Atlantic and tropical Pacific, *Prog. Oceanogr.*, 73, 127–144, doi:10.1016/j.pocean.2007.02.003, 2007.
- 30 Devred, E., Sathyendranath, S., and Platt, T.: Delineation of ecological provinces using ocean colour radiometry, *Mar. Ecol.-Prog. Ser.*, 346, 1–13, doi:10.3354/meps07149, 2007.

- Dietze, H., Oschlies, A., and Kahler, P.: Internal-wave-induced and double-diffusive nutrient fluxes to the nutrient-consuming surface layer in the oligotrophic subtropical North Atlantic, *Ocean Dynam.*, 54, 1–7, doi:10.1007/s10236-003-0060-9, 2004.
- Edler, L.: Recommendations for Marine Biological Studies in the Baltic Sea: Phytoplankton and Chlorophyll, *Baltic Marine Biologists* (Eds.), Publication No. 3, 1979.
- Fahrbach, E., Rohardt, G., and Sieger, R.: 25 Years of Polarstern Hydrography (1982–2007), *WDC-MARE Reports*, 5, 88 pp., 2007.
- Ferrari, G. M. and Tassan, S.: A method using chemical oxidation to remove light absorption by phytoplankton pigments, *J. Phycol.*, 35, 1090–1098, 1999.
- Gibb, S. W., Barlow, R. G., Cummings, D. G., Rees, N. W., Trees, C. C., Holligan, P., and Suggett, D.: Surface phytoplankton pigment distributions in the Atlantic Ocean: an assessment of basin scale variability between 50 degrees N and 50 degrees S, *Prog. Oceanogr.*, 45, 339–368, 2000.
- Goericke, R. and Repeta, D. J.: The pigments of *Prochlorococcus marinus* – The presence of divinyl chlorophyll *a* and chlorophyll *b* in a marine prokaryote, *Limnol. Oceanogr.*, 37, 425–433, 1992.
- Hardman-Mountford, N. J., Hirata, T., Richardson, K. A., and Aiken, J.: An objective methodology for the classification of ecological pattern into biomes and provinces for the pelagic ocean, *Remote Sens. Environ.*, 112, 3341–3352, doi:10.1016/j.rse.2008.02.016, 2008.
- Heywood, J. L., Zubkov, M. V., Tarran, G. A., Fuchs, B. M., and Holligan, P. M.: Prokaryoplankton standing stocks in oligotrophic gyre and equatorial provinces of the Atlantic Ocean: Evaluation of inter-annual variability, *Deep-Sea Res. Pt. II*, 53, 1530–1547, doi:10.1016/j.dsr2.2006.05.005, 2006.
- Hoffmann, L. J., Peeken, I., Lochte, K., Assmy, P., and Veldhuis, M.: Different reactions of Southern Ocean phytoplankton size classes to iron fertilization, *Limnol. Oceanogr.*, 51, 1217–1229, 2006.
- Hooker, S. B., Rees, N. W., and Aiken, J.: An objective methodology for identifying oceanic provinces, *Prog. Oceanogr.*, 45, 313–338, 2000.
- Jeffrey, S. W., Mantoura, R. F. C., and Wright, S. W.: *Phytoplankton Pigments in Oceanography, Guidelines to Modern Methods*, 2nd Edn., UNESCO Publishing, Paris, 2005.
- Johnson, Z. I., Zinser, E. R., Coe, A., McNulty, N. P., Woodward, E. M. S., and Chisholm, S. W.: Niche partitioning among *Prochlorococcus* ecotypes along ocean-scale environmental gradients, *Science*, 311, 1737–1740, 2006.

---

**Bio-optical provinces  
in the eastern  
Atlantic Ocean**B. B. Taylor et al.

---

[Title Page](#)[Abstract](#)[Introduction](#)[Conclusions](#)[References](#)[Tables](#)[Figures](#)[◀](#)[▶](#)[◀](#)[▶](#)[Back](#)[Close](#)[Full Screen / Esc](#)[Printer-friendly Version](#)[Interactive Discussion](#)

---

## Bio-optical provinces in the eastern Atlantic Ocean

---

B. B. Taylor et al.

[Title Page](#)
[Abstract](#)
[Introduction](#)
[Conclusions](#)
[References](#)
[Tables](#)
[Figures](#)
[Back](#)
[Close](#)
[Full Screen / Esc](#)
[Printer-friendly Version](#)
[Interactive Discussion](#)


- Koch, B. P. and Kattner, G.: Sources and short-term molecular changes of dissolved organic matter in the Atlantic Surface Ocean, *Biogeosciences*, submitted, 2011.
- Kolber, Z. S., Prasil, O., and Falkowski, P. G.: Measurements of variable chlorophyll fluorescence using fast repetition rate techniques: defining methodology and experimental protocols, *Biochim. Biophys. Acta*, 1367, 88–106, 1998.
- Letelier, R. M., Bidigare, R. R., Hebel, D. V., Ondrusek, M., Winn, C. D., and Karl, D. M.: Temporal variability of phytoplankton community structure-based on pigment analysis, *Limnol. Oceanogr.*, 38, 1420–1437, 1993.
- Levitus, S.: *Climatological Atlas of the World Ocean*, NOAA Professional Paper 13, U.S. Department of Commerce, 1982.
- Li, W. K. W. and Harrison, W. G.: Chlorophyll, bacteria and picophytoplankton in ecological provinces of the North Atlantic, *Deep-Sea Res. Pt. II*, 48, 2271–2293, 2001.
- Li, W. K. W.: From cytometry to macroecology: a quarter century quest in microbial oceanography, *Aquat. Microb. Ecol.*, 57, 239–251, doi:10.3354/ame01328, 2009.
- Longhurst, A.: *Ecological Geography of the Sea*, 2nd Edn., Elsevier Academic Press, USA, 2007.
- Lubac, B. and Loisel, H.: Variability and classification of remote sensing reflectance spectra in the eastern English Channel and southern North Sea, *Remote Sens. Environ.*, 110, 45–48, 2007.
- Mackey, M. D., Mackey, D. J., Higgins, H. W., and Wright, S. W.: CHEMTAX – A program for estimating class abundances from chemical markers: Application to HPLC measurements of phytoplankton, *Mar. Ecol.-Prog. Ser.*, 144, 265–283, 1996.
- Marañón, E., Holligan, P. M., Varela, M., Mourino, B., and Bale, A. J.: Basin-scale variability of phytoplankton biomass, production and growth in the Atlantic Ocean, *Deep-Sea Res. Pt. I*, 47, 825–857, 2000.
- Marañón, E., Holligan, P. M., Barciela, R., Gonzalez, N., Mourino, B., Pazo, M. J., and Varela, M.: Patterns of phytoplankton size structure and productivity in contrasting open-ocean environments, *Mar. Ecol.-Prog. Ser.*, 216, 43–56, 2001.
- Margalef, R.: Life-forms of phytoplankton as survival alternatives in an unstable environment, *Oceanol. Acta*, 1, 493–509, 1978.
- Marie, D., Simon, N., and Vaulot, D.: Phytoplankton cell counting by flow cytometry, in: *Algal Culturing Techniques*, edited by: Andersen, R. A., Elsevier Academic Press, 2005.
- Maritorena, S. and Siegel, D. A.: Consistent merging of satellite ocean color data sets using

---

## Bio-optical provinces in the eastern Atlantic Ocean

B. B. Taylor et al.

---

Title Page

Abstract

Introduction

Conclusions

References

Tables

Figures

◀

▶

◀

▶

Back

Close

Full Screen / Esc

Printer-friendly Version

Interactive Discussion



a bio-optical model, *Remote Sens. Environ.*, 94, 429–440, doi:10.1016/j.rse.2004.08.014, 2005.

Maritorena, S., d’Andon, O. H. F., Mangin, A., and Siegel, D. A.: Merged satellite ocean color data products using a bio-optical model: Characteristics, benefits and issues, *Remote Sens. Environ.*, 114, 1791–1804, doi:10.1016/j.rse.2010.04.002, 2010.

Matsuoka, A., Hout, Y., Shimada, K., Saitoh, S., and Babin, M.: Bio-optical characteristics of the western Arctic Ocean: implications for ocean color algorithms, *Can. J. Remote Sens.*, 33, 503–518, 2007.

McClain, C. R.: A Decade of Satellite Ocean Color Observations, *Annual Review of Marine Science*, 1, 19–42, doi:10.1146/annurev.marine.010908.163650, 2009.

McGillicuddy, D. J., Anderson, L. A., Doney, S. C., and Maltrud, M. E.: Eddy-driven sources and sinks of nutrients in the upper ocean: Results from a 0.1 degrees resolution model of the North Atlantic, *Global Biogeochem. Cy.*, 17, 1035, doi:10.1029/2002gb001987, 2003.

Mills, M. M., Ridame, C., Davey, M., La Roche, J., and Geider, R. J.: Iron and phosphorus co-limit nitrogen fixation in the eastern tropical North Atlantic, *Nature*, 429, 292–294, doi:10.1038/nature02550, 2004.

Moore, L. R. and Chisholm, S. W.: Photophysiology of the marine cyanobacterium *Prochlorococcus*: Ecotypic differences among cultured isolates, *Limnol. Oceanogr.*, 44, 628–638, 1999.

Mueller, J. L., Fargion, G. S., and McClain, C. R.: Ocean Optics Protocols for Satellite Ocean Color Sensor Validation, Revision 4, Volume III: Radiometric Measurements and Data Analysis Protocols, NASA/TM-2003-211621/Rev4-Vol. III, NASA Goddard Space Flight Center, Greenbelt, Maryland, 2003.

Neogi, S. B., Koch, B. P., Schmitt-Kopplin, P., Pohl, C., Kattner, G., Yamasaki, S., and Lara, R. J.: Biogeochemical controls on the bacterial population in the eastern Atlantic Ocean, *Biogeosciences*, submitted, 2011.

Oksanen, J., Blanchet, F. G., Kindt, R., Legendre, P., O’Hara, R. B., Simpson, G. L., Solymos, P., Stevens, M. H. H., and Wagner, H.: *vegan*: Community Ecology Package. R package version 1.17-4: <http://CRAN.R-project.org/package=vegan>, 2010.

Oschlies, A., Dietze, H., and Kahler, P.: Salt-finger driven enhancement of upper ocean nutrient supply, *Geophysical Res. Lett.*, 30, 2204, doi:10.1029/2003gl018552, 2003.

Partensky, F. and Garczarek, L.: *Prochlorococcus*: Advantages and Limits of Minimalism, *Annual Review of Marine Science*, 2, 305–331, doi:10.1146/annurev-marine-120308-081034,

2010.

Partensky, F., Hess, W. R., and Vaultot, D.: *Prochlorococcus*, a marine photosynthetic prokaryote of global significance, *Microbiol. Mol. Biol. R.*, 63, 106–127, 1999.

Pérez, V., Fernandez, E., Marañón, E., Serret, P., Varela, R., Bode, A., Varela, M., Varela, M. M., Moran, X. A. G., Woodward, E. M. S., Kitidis, V., and Garcia-Soto, C.: Latitudinal distribution of microbial plankton abundance, production, and respiration in the Equatorial Atlantic in Autumn 2000, *Deep-Sea Res. Pt. I*, 52, 861–880, doi:10.1016/j.dsr.2005.01.002, 2005.

Platt, T. and Sathyendranath, S.: Spatial structure of pelagic ecosystem processes in the global ocean, *Ecosystems*, 2, 384–394, 1999.

Platt, T., Bouman, H., Devred, E., Fuentes-Yaco, C., and Sathyendranath, S.: Physical forcing and phytoplankton distributions, *Sci. Mar.*, 69, 55–73, 2005.

Pohl, C., Croot, P. L., Hennings, U., Daberkow, T., Budeus, G., and Loeff, M. R. v. d.: Synoptic transects on the distribution of trace elements (Hg, Pb, Cd, Cu, Ni, Zn, Co, Mn, Fe, and Al) in surface waters of the Northern- and Southern East Atlantic, *J. Marine Syst.*, 84, 28–41, 2011.

R Development Core Team: R: A Language and Environment for Statistical Computing, R Foundation for Statistical Computing, Vienna, Austria, ISBN 3-900051-07-0, <http://www.R-project.org>, 2008.

Richardson, P. L., Bower, A. S., and Zenk, W.: A census of Meddies tracked by floats, *Prog. Oceanogr.*, 45, 209–250, 2000.

Rohardt, G.: Continuous thermosalinograph oceanography along POLARSTERN cruise track ANT-XXV/1, Alfred Wegener Institute for Polar and Marine Research, Bremerhaven, doi:10.1594/PANGAEA.727470, 2009.

Saba, V. S., Friedrichs, M. A. M., Antoine, D., Armstrong, R. A., Asanuma, I., Behrenfeld, M. J., Ciotti, A. M., Dowell, M., Hoepffner, N., Hyde, K. J. W., Ishizaka, J., Kameda, T., Marra, J., Mélin, F., Morel, A., O'Reilly, J., Scardi, M., Smith Jr., W. O., Smyth, T. J., Tang, S., Uitz, J., Waters, K., and Westberry, T. K.: An evaluation of ocean color model estimates of marine primary productivity in coastal and pelagic regions across the globe, *Biogeosciences*, 8, 489–503, doi:10.5194/bg-8-489-2011, 2011.

Sarthou, G., Baker, A. R., Blain, S., Achterberg, E. P., Boye, M., Bowie, A. R., Croot, P., Laan, P., de Baar, H. J. W., Jickells, T. D., and Worsfold, P. J.: Atmospheric iron deposition and sea-surface dissolved iron concentrations in the eastern Atlantic Ocean, *Deep-Sea Res. Pt. I*, 50,

**BGD**

8, 7165–7219, 2011

---

## Bio-optical provinces in the eastern Atlantic Ocean

B. B. Taylor et al.

---

Title Page

Abstract

Introduction

Conclusions

References

Tables

Figures

◀

▶

◀

▶

Back

Close

Full Screen / Esc

Printer-friendly Version

Interactive Discussion



---

## Bio-optical provinces in the eastern Atlantic Ocean

B. B. Taylor et al.

---

Title Page

Abstract

Introduction

Conclusions

References

Tables

Figures

◀

▶

◀

▶

Back

Close

Full Screen / Esc

Printer-friendly Version

Interactive Discussion



1339–1352, doi:10.1016/s0967-0637(03)00126-2, 2003.

Sathyendranath, S., Platt, T., Horne, E. P. W., Harrison, W. G., Ulloa, O., Outerbridge, R., and Hoepffner, N.: Estimation of new production in the ocean by compound remote-sensing, *Nature*, 353, 129–133, 1991.

5 Sathyendranath, S., Longhurst, A., Caverhill, C. M., and Platt, T.: Regionally and seasonally differentiated primary production in the North Atlantic, *Deep-Sea Res. Pt. I*, 42, 1773–1802, 1995.

Sathyendranath, S., Cota, G., Stuart, V., Maass, H., and Platt, T.: Remote sensing of phytoplankton pigments: a comparison of empirical and theoretical approaches, *Int. J. Remote Sens.*, 22, 249–273, 2001.

10 Siedler, G., Armi, L., and Muller, T. J.: Meddies and decadal changes at the Azores Front from 1980 to 2000, *Deep-Sea Res. Pt. II*, 52, 583–604, doi:10.1016/j.dsr2.2004.12.010, 2005.

Simis, S. G. H., Tijdens, M., Hoogveld, H. L., and Gons, H. J.: Optical changes associated with cyanobacterial bloom termination by viral lysis, *J. Plankton Res.*, 27, 937–949, doi:10.1093/plankt/fbi068, 2005.

15 Stramski, D., Reynolds, R. A., Babin, M., Kaczmarek, S., Lewis, M. R., Röttgers, R., Sciandra, A., Stramska, M., Twardowski, M. S., Franz, B. A., and Claustre, H.: Relationships between the surface concentration of particulate organic carbon and optical properties in the eastern South Pacific and eastern Atlantic Oceans, *Biogeosciences*, 5, 171–201, doi:10.5194/bg-5-171-2008, 2008.

20 Strass, V. H.: Meridional and seasonal variations in the satellite-sensed fraction of euphotic zone chlorophyll, *J. Geophys. Res.-Oceans*, 95/C10, 18289–18301, 1990.

Switzer, A. C., Kamykowski, D., and Zentara, S. J.: Mapping nitrate in the global ocean using remotely sensed sea surface temperature, *J. Geophys. Res.-Oceans*, 108, 3280, doi:10.1029/2000jc000444, 2003.

25 Tarran, G. A., Heywood, J. L., and Zubkov, M. V.: Latitudinal changes in the standing stocks of nano- and picoeukaryotic phytoplankton in the Atlantic Ocean, *Deep-Sea Res. Pt. II*, 53, 1516–1529, doi:10.1016/j.dsr2.2006.05.004, 2006.

Tassan, S. and Ferrari, G. M.: An alternative approach to absorption measurements of aquatic particles retained on filters, *Limnol. Oceanogr.*, 40, 1358–1368, 1995.

30 Torrecilla, E., Piera, J., Bracher, A., Taylor, B. B., and Bernhardt, A.: Spectral range sensitivity analysis to improve hyperspectral remote sensing of phytoplankton biodiversity in the ocean, *IEEE Third Workshop on Hyperspectral Image and Signal Processing: Evolution in Remote*

## Bio-optical provinces in the eastern Atlantic Ocean

B. B. Taylor et al.

Title Page

Abstract

Introduction

Conclusions

References

Tables

Figures

◀

▶

◀

▶

Back

Close

Full Screen / Esc

Printer-friendly Version

Interactive Discussion



- Sensing, WHIPSERS'11, Lisbon, Portugal, 2011a.
- Torrecilla, E., Stramski, D., Reynolds, R. A., Millán-Núñez, E., and Piera, J.: Cluster analysis of hyperspectral optical data for discriminating phytoplankton pigment assemblages in the open ocean, *Remote Sens. Environ.*, in press, 2011b.
- 5 Uitz, J., Claustre, H., Morel, A., and Hooker, S. B.: Vertical distribution of phytoplankton communities in open ocean: An assessment based on surface chlorophyll, *J. Geophys. Res.-Oceans*, 111, C08005, doi:10.1029/2005jc003207, 2006.
- Utermöhl, H: Zur Vervollkommnung der quantitativen Phytoplankton-Methodik, *Internationale Vereinigung für Theoretische und Angewandte Limnologie (Eds.)*, Publication No. 9, 1958.
- 10 Veldhuis, M. J. W. and Kraay, G. W.: Phytoplankton in the subtropical Atlantic Ocean: towards a better assessment of biomass and composition, *Deep-Sea Res. Pt. I*, 51, 507–530, doi:10.1016/j.dsr.2003.12.002, 2004.
- Vesk, M. and Jeffrey, S. W.: Ultrastructure and pigments of 2 strains of the picoplanktonic alga *Pelagococcus subviridis* (Chrysophyceae), *J. Phycol.*, 23, 322–336, 1987.
- 15 Vidussi, F., Claustre, H., Manca, B. B., Luchetta, A., and Marty, J. C.: Phytoplankton pigment distribution in relation to upper thermocline circulation in the eastern Mediterranean Sea during winter, *J. Geophys. Res.-Oceans*, 106, 19939–19956, 2001.
- VLIZ: Longhurst Biogeographical Provinces: <http://www.vliz.be/vmdcdata/vlimar/downloads.php>, access: 3 November 2010, 2009.
- 20 Wang, X. J., Behrenfeld, M., Le Borgne, R., Murtugudde, R., and Boss, E.: Regulation of phytoplankton carbon to chlorophyll ratio by light, nutrients and temperature in the Equatorial Pacific Ocean: a basin-scale model, *Biogeosciences*, 6, 391–404, doi:10.5194/bg-6-391-2009, 2009.
- Wernand, M. R.: Guidelines for (ship-borne) auto-monitoring of coastal and ocean color, *Ocean Optics XVI*, Santa Fe, New Mexico, US, 2002.
- 25 West, N. J. and Scanlan, D. J.: Niche-partitioning of *Prochlorococcus* populations in a stratified water column in the eastern North Atlantic Ocean, *Appl. Environ. Microbiol.*, 65, 2585–2591, 1999.
- Wright, S. W. and Jeffrey, S. W.: Fucoxanthin pigment markers of marine phytoplankton analyzed by HPLC and HPTLC, *Mar. Ecol.-Prog. Ser.*, 38, 259–266, 1987.
- 30 Zinser, E. R., Johnson, Z. I., Coe, A., Karaca, E., Veneziano, D., and Chisholm, S. W.: Influence of light and temperature on *Prochlorococcus* ecotype distributions in the Atlantic Ocean, *Limnol. Oceanogr.*, 52, 2205–2220, 2007.

Zubkov, M. V., Sleigh, M. A., Tarran, G. A., Burkill, P. H., and Leakey, R. J. G.: Picoplanktonic community structure on an Atlantic transect from 50 degrees N to 50 degrees S, Deep-Sea Res. Pt. I, 45, 1339–1355, 1998.

5 Zubkov, M. V., Sleigh, M. A., and Burkill, P. H.: Assaying picoplankton distribution by flow cytometry of underway samples collected along a meridional transect across the Atlantic Ocean, Aquat. Microb. Ecol., 21, 13–20, 2000.

Zwirgmaier, K., Heywood, J. L., Chamberlain, K., Woodward, E. M. S., Zubkov, M. V., and Scanlan, D. J.: Basin-scale distribution patterns of picocyanobacterial lineages in the Atlantic Ocean, Environ. Microbiol., 9, 1278–1290, doi:10.1111/j.1462-2920.2007.01246.x, 2007.

**BGD**

8, 7165–7219, 2011

---

**Bio-optical provinces  
in the eastern  
Atlantic Ocean**

B. B. Taylor et al.

---

Title Page

Abstract

Introduction

Conclusions

References

Tables

Figures

◀

▶

◀

▶

Back

Close

Full Screen / Esc

Printer-friendly Version

Interactive Discussion



## Bio-optical provinces in the eastern Atlantic Ocean

B. B. Taylor et al.

**Table 1.** Solvent gradient used for HPLC measurements. Solvent A: 30 % 1 mol L<sup>-1</sup> ammonium acetate, 70 % methanol. Solvent B: 100 % methanol.

Gradient [min]	Flow [ml min <sup>-1</sup> ]	% Solvent A	% Solvent B	Curve
0	1	65	35	
1	1	40	60	6
7	1	15	85	6
13	1	0	100	10
19	1	0	100	6
20	1	65	35	6

Title Page

Abstract

Introduction

Conclusions

References

Tables

Figures

◀

▶

◀

▶

Back

Close

Full Screen / Esc

Printer-friendly Version

Interactive Discussion



## Bio-optical provinces in the eastern Atlantic Ocean

B. B. Taylor et al.

Title Page

Abstract

Introduction

Conclusions

References

Tables

Figures

◀

▶

◀

▶

Back

Close

Full Screen / Esc

Printer-friendly Version

Interactive Discussion



**Table 2.** List of pigments analysed in this study, their abbreviations used in the text and associated phytoplankton groups, if the pigment is used as a marker pigment in literature. Pigments which have no associated phytoplankton group in this table are not specific for one group.

Pigment	Abbreviation	Diagnostic pigment for	Key references
Alloxanthin	Allo	Cryptophyceae	3, 4
Astaxanthin	Asta		
<i>Monovinyl</i> -Chlorophyll- <i>a</i>	Chl- <i>a</i>		
<i>Divinyl</i> -Chlorophyll- <i>a</i>	DV <i>a</i>	<i>Prochlorococcus</i> sp.	1, 5, 6, 7
<i>Monovinyl</i> -Chlorophyll- <i>b</i>	Chl- <i>b</i>	Green algae	4
<i>Divinyl</i> -Chlorophyll- <i>b</i>	DV <i>b</i>	<i>Prochlorococcus</i> sp.	1, 5, 6, 7
Chlorophyll- <i>c</i> <sub>1/2</sub>	Chl- <i>c</i> <sub>1/2</sub>		
Chlorophyll- <i>c</i> <sub>3</sub>	Chl- <i>c</i> <sub>3</sub>		
$\alpha$ -carotene	$\alpha$ -car		
$\beta$ -carotene	$\beta$ -car		
Diadinoxanthin	Diadino		
Diatoxanthin	Diato		
Fucoxanthin	Fuco	Bacillariophyceae	2, 5, 8
19'-hexanoyloxyfucoxanthin	19 HF	Haptophytes	2, 4, 5
19'-butanoyloxyfucoxanthin	19 BF	Chrysophyceae	2, 4, 5
Neoxanthin	Neo		
Lutein	Lut		
Peridinin	Peri	Dinophyceae	2, 5
Phaeophytin- <i>a</i>	Phyt- <i>a</i>		
Phaeophytin- <i>b</i>	Phyt- <i>b</i>		
Prasincoxanthin	Prasino	Prasinophyceae	2, 5
Violaxanthin	Viola		
Zeaxanthin	Zea	Cyanophyceae	1, 4, 7, 8

1: Goericke and Repeta (1992); 2: Letelier et al. (1993); 3: Pennington et al. (1985); 4: Jeffrey et al. (2005); 5: Björnland and Liaanen-Jensein (1989); 6: Partensky et al. (1993); 7: Morel et al. (1993); 8: Gieskes et al. (1988).

## Bio-optical provinces in the eastern Atlantic Ocean

B. B. Taylor et al.

Title Page

Abstract

Introduction

Conclusions

References

Tables

Figures

◀

▶

◀

▶

Back

Close

Full Screen / Esc

Printer-friendly Version

Interactive Discussion



**Table 3.** Best correlated environmental variables to pigment composition identified by the BIO-ENV routine.

<i>N</i>	Factors	$\rho$
1	Temp	0.235
2	Lat + Temp	0.266
3	Lat + Temp + Sal	0.213

*N* = number of factors;  $\rho$  = Spearman rank correlation coefficient.

## Bio-optical provinces in the eastern Atlantic Ocean

B. B. Taylor et al.

Title Page

Abstract

Introduction

Conclusions

References

Tables

Figures

◀

▶

◀

▶

Back

Close

Full Screen / Esc

Printer-friendly Version

Interactive Discussion



**Table 4.** Best correlated pigments to pigment composition identified by the BIO-BIO routine.

<i>N</i>	Factors	$\rho$
1	DVa	0.734
2	DVa + Zea	0.847
3	DVa + Zea + Fuco	0.919
4	DVa + Zea + Fuco + DVb	0.958
5	DVa + Zea + Fuco + DVb + Chl- <i>a</i>	0.984

*N* = number of factors;  $\rho$  = Spearman rank correlation coefficient.

## Bio-optical provinces in the eastern Atlantic Ocean

B. B. Taylor et al.

Title Page

Abstract

Introduction

Conclusions

References

Tables

Figures

◀

▶

◀

▶

Back

Close

Full Screen / Esc

Printer-friendly Version

Interactive Discussion



**Table 5.** Cophenetic indices between pigment-based and optical-based cluster trees obtained using different spectral ranges of  $a_{\text{ph}}(\lambda)$  and  $R_{\text{rs}}(\lambda)$ . In the case of the remote sensing reflectance data, the 2nd derivative was used to obtain a better cophenetic index.

	Cophenetic index
Phytoplankton absorption data – $a_{\text{ph}}(\lambda)$	
Hyperspectral (1 nm resolution), range 350–750 nm	0.454
Hyperspectral (1 nm resolution), range 435–520 nm	0.703
Remote-sensing reflectance data – $R_{\text{rs}}(\lambda)$	
Hyperspectral (1 nm resolution), range 350–750 nm	0.330
Hyperspectral (1 nm resolution), range 435–580 nm	0.498
Hyperspectral 2nd derivative, range 435–580 nm	0.625
Optimal derivative parameters: BS = 9, WS = 9	

**Table 6.** Summary of cluster properties.

Clus.	Stat.	Dom. Pig.	Tchl- <i>a</i> [mg m <sup>-3</sup> ]	Temp. [°C]	Salinity	DCM [m]	Z <sub>eu</sub> [m]	Z <sub>m</sub> [m]	Longh. Prov.
I	1	Fuco, Chl- <i>b</i>	0.73 <sup>1</sup>	14.18 <sup>1</sup>	35.31 <sup>1</sup>	No DCM	n.d.	mixed	NECS
II	2	Chl- <i>b</i> , 19 HF	2.06 <sup>1</sup>	13.32 <sup>1</sup>	35.42 <sup>1</sup>	No DCM	n.d.	56 <sup>1</sup>	NECS (tidal front)
III	3–5, 7, 22	19 HF	0.60±0.26	17.39±3.26	35.08±0.29	No DCM	68 <sup>1</sup>	67, 96 (2 profiles)	NADR (and others)
IV-N	6, 8–10, 14–16, 18	Zea, DV <sub>a</sub> , 19 HF	0.34±0.16 <sup>2</sup>	19.71±2.10 <sup>2</sup>	36.62±0.35 <sup>2</sup>	76.8±20.6	88.7±6.6	77.3±11.0 <sup>2</sup>	NAST (E)
IV-S	26–37, 39–40	Zea, DV <sub>a</sub> , 19 HF	0.22±0.06	26.82±2.32	35.56±0.77	59.3±8.8	84.9±15.5	33.6±17.7	ETRA
V	21, 24–25	Fuco, Diad, Chl- <i>c</i> <sub>1/2</sub>	3.24±1.66	25.27±2.65	36.01±0.39	37 <sup>1</sup>	35 <sup>1</sup>	13 <sup>1</sup>	Blooms (CNRY?)
VI	41–48	Zea, 19 HF	0.32±0.09	19.55±0.48	35.99±0.25	39.5±7.3	63.3±8.7	33.3±16.1	SATL
Outliers	11, 13	Zea, DV <sub>a</sub> , DV <sub>b</sub>	0.10	20.24	36.91	n.d.	n.d.	n.d.	NAST (E)
			0.16	20.73	36.96				
	12	DV <sub>b</sub> , DV <sub>a</sub> , 19 HF	0.23	20.66	36.97	n.d.	n.d.	n.d.	NAST (E)
		Fuco, DV <sub>a</sub> , Zea	0.64	22.98	36.90	n.d.	n.d.	n.d.	NATR?
	19, 20		0.82	23.11	37.00				
		0.19	23.42	36.21	n.d.	n.d.	n.d.	ETRA	

Clus. = Clusters; Stat. = Stations; Dom. Pig. = Dominant pigments (in addition to chl-*a*) common to all stations within the cluster; Tchl-*a* = chl-*a* + DV<sub>a</sub> (Mean±SD); Temp. = Surface temperature (Mean±SD); Salinity = Surface salinity (Mean±SD); DCM = Deep Chlorophyll Maximum; Z<sub>eu</sub> = euphotic depth; Z<sub>m</sub> = Mixed layer depth (sigma); Longh. Prov. = assigned Longhurst Provinces: NECS = Northeast Atlantic Shelves Province, NADR = North Atlantic Drift Province, NAST (E) = North Atlantic Subtropical Gyral Province (East), ETRA = Eastern Tropical Atlantic Province, CNRY = Canary Current Coastal Province, SATL = South Atlantic Gyral Province; n.d. = no data.

<sup>1</sup> one data point or one profile only, <sup>2</sup> significantly different from sub-cluster IV-S ( $p < 0.05$ ).

Title Page

Abstract

Introduction

Conclusions

References

Tables

Figures

◀

▶

◀

▶

Back

Close

Full Screen / Esc

Printer-friendly Version

Interactive Discussion



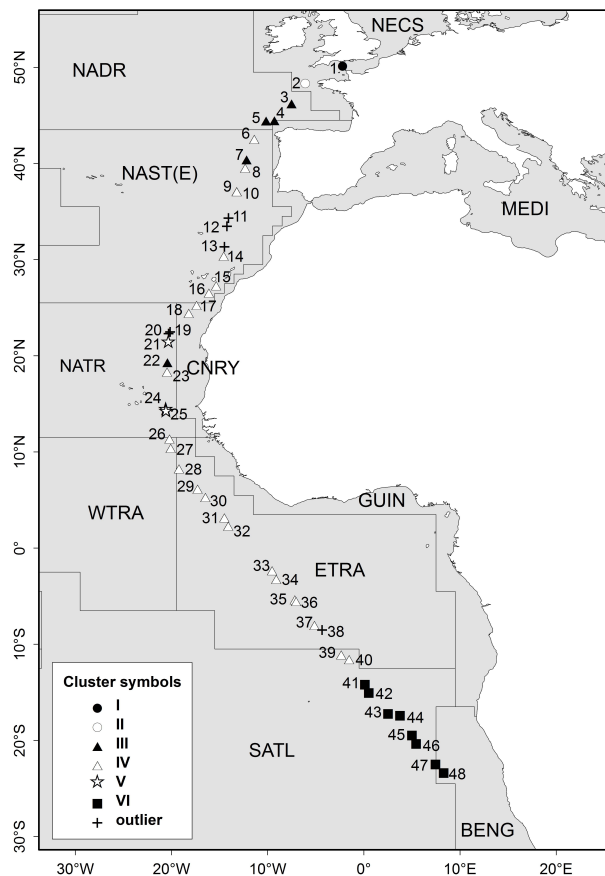


**Fig. 1.** Map of study area, showing the sample stations during cruise ANT XXV-1 on R/V *Polarstern* in November 2008 overlying the oceanic provinces defined by Longhurst (2007). The symbols represent the pigment-based clusters defined in Fig. 4.

**Bio-optical provinces  
in the eastern  
Atlantic Ocean**

B. B. Taylor et al.

Title Page

Abstract

Introduction

Conclusions

References

Tables

Figures

◀

▶

◀

▶

Back

Close

Full Screen / Esc

Printer-friendly Version

Interactive Discussion



## Bio-optical provinces in the eastern Atlantic Ocean

B. B. Taylor et al.

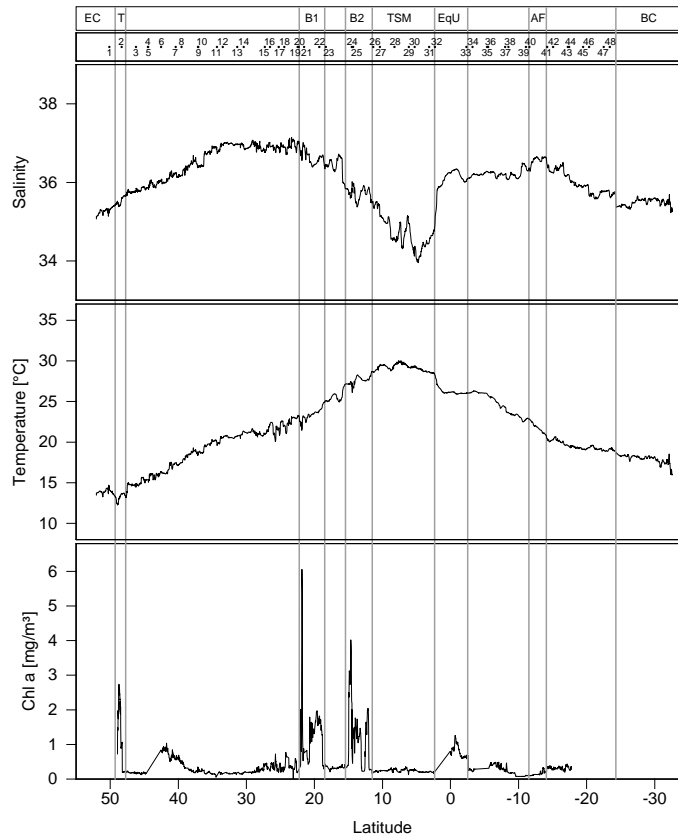


**Fig. 2.** Major oceanographic features of the transect, dots at the top depict the locations and numbers of the stations where water samples were taken, (EC = English Channel, T = Tidal Front, B1 = Bloom No. 1, B2 = Bloom No. 2, TSM = Tropical Salinity Minimum Zone, EqU = Equatorial Upwelling, AF = Angola-Benguela Front, BC = Benguela Current), reproduced with own data after Sarthou et al. (2003).

Title Page

Abstract

Introduction

Conclusions

References

Tables

Figures

◀

▶

◀

▶

Back

Close

Full Screen / Esc

Printer-friendly Version

Interactive Discussion



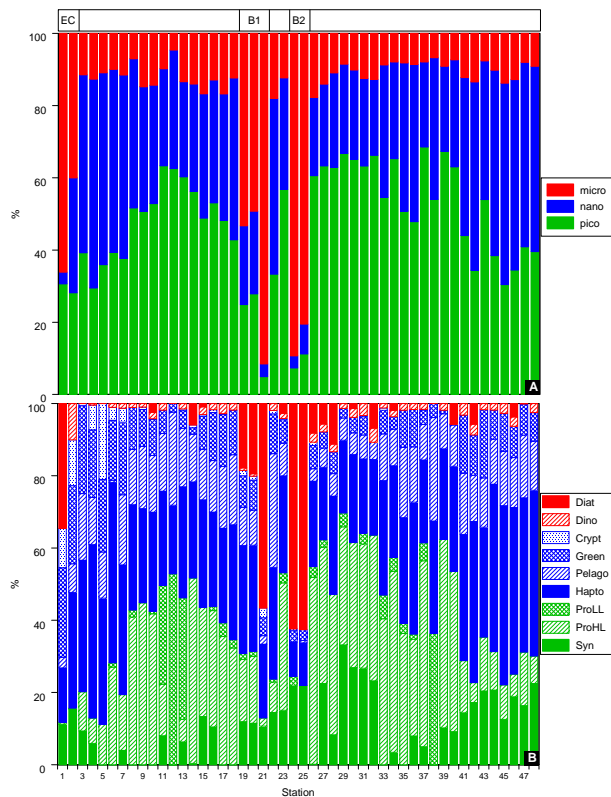


**Fig. 3.** Phytoplankton composition calculated from pigment composition **(A)** size classes approach (micro = microplankton, nano = nanoplankton, pico = picoplankton) **(B)** CHEM-TAX approach (Diat = Diatoms, Dino = Dinoflagellates, Crypt = Cryptophytes, Green = Green algae, Pelago = Pelagophyceae, Hapto = Haptophytes, ProLL = *Prochlorococcus* low-light adapted, ProHL = *Prochlorococcus* high-light adapted, Syn = *Synechococcus*-type cyanobacteria, EC = English Channel, B1 = Bloom No. 1, B2 = Bloom No. 2).

**Bio-optical provinces  
in the eastern  
Atlantic Ocean**

B. B. Taylor et al.

Title Page

Abstract Introduction

Conclusions References

Tables Figures

◀ ▶

◀ ▶

Back Close

Full Screen / Esc

Printer-friendly Version

Interactive Discussion



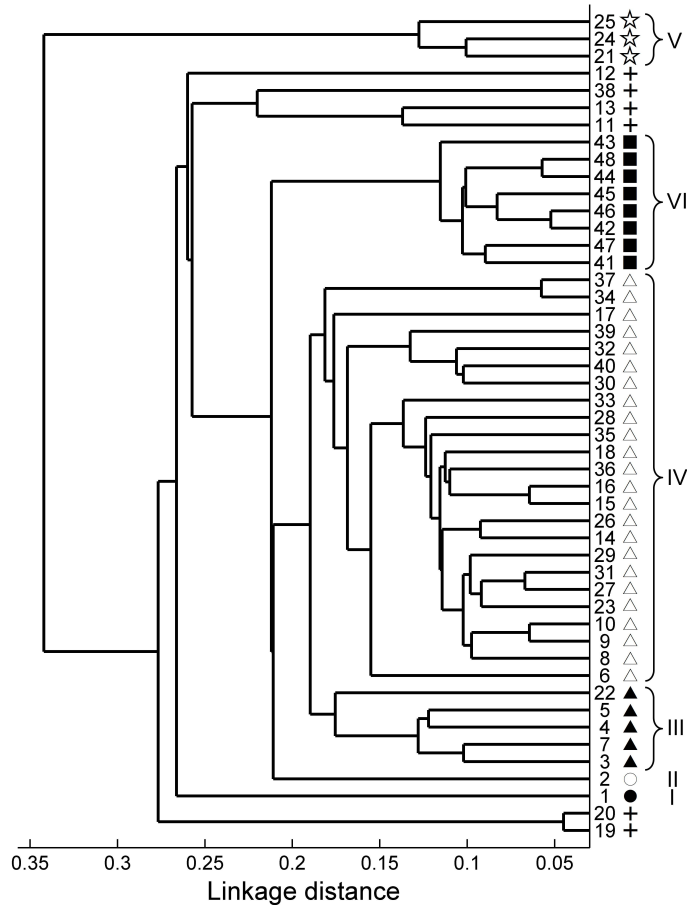


**Fig. 4.** Cluster tree of stations based on hierarchical cluster analysis of pigment data. Each cluster (assigned at a linkage distance of 0.18) has been assigned a different symbol and roman number.

**Bio-optical provinces  
in the eastern  
Atlantic Ocean**

B. B. Taylor et al.

Title Page

Abstract

Introduction

Conclusions

References

Tables

Figures

◀

▶

◀

▶

Back

Close

Full Screen / Esc

Printer-friendly Version

Interactive Discussion



## Bio-optical provinces in the eastern Atlantic Ocean

B. B. Taylor et al.

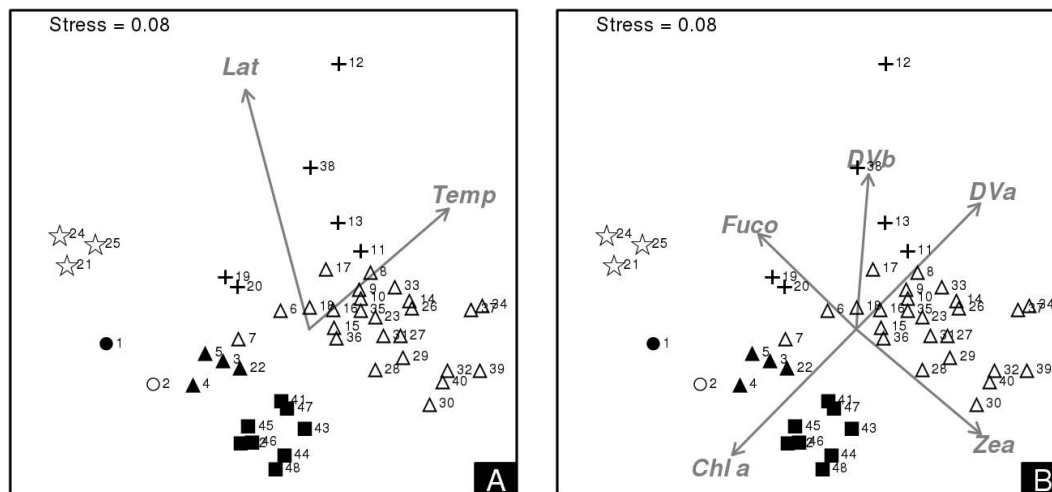


**Fig. 5.** Multi-dimensional scaling (MDS) plots visualizing sample similarities in terms of pigment composition. Symbols represent pigment-based clusters defined in Fig. 4. Additional vectors were fit to the MDS ordination for the environmental factors (A) and pigments (B) identified by the BIO-ENV and BIO-BIO routines. The fitted vectors have maximum correlation with the corresponding variables.

Title Page

Abstract

Introduction

Conclusions

References

Tables

Figures

◀

▶

◀

▶

Back

Close

Full Screen / Esc

Printer-friendly Version

Interactive Discussion



**Fig. 6.** Cluster tree of stations based on phytoplankton absorption ( $a_{ph}(\lambda)$ ). Symbols correspond to pigment-based clusters (Fig. 4).

**Bio-optical provinces  
in the eastern  
Atlantic Ocean**

B. B. Taylor et al.

Title Page

Abstract Introduction

Conclusions References

Tables Figures

◀ ▶

◀ ▶

Back Close

Full Screen / Esc

Printer-friendly Version

Interactive Discussion



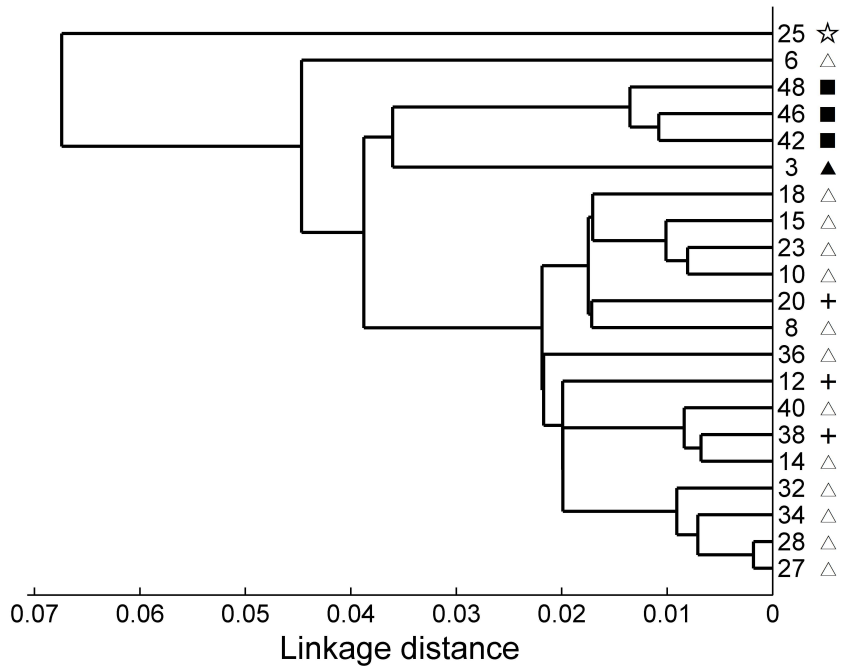


**Fig. 7.** Cluster tree of stations based on remote sensing reflectance ( $R_{rs}(\lambda)$ ). Symbols correspond to pigment-based clusters (Fig. 4).

**Bio-optical provinces  
in the eastern  
Atlantic Ocean**

B. B. Taylor et al.

Title Page

Abstract Introduction

Conclusions References

Tables Figures

◀ ▶

◀ ▶

Back Close

Full Screen / Esc

Printer-friendly Version

Interactive Discussion



Bio-optical provinces  
in the eastern  
Atlantic Ocean

B. B. Taylor et al.

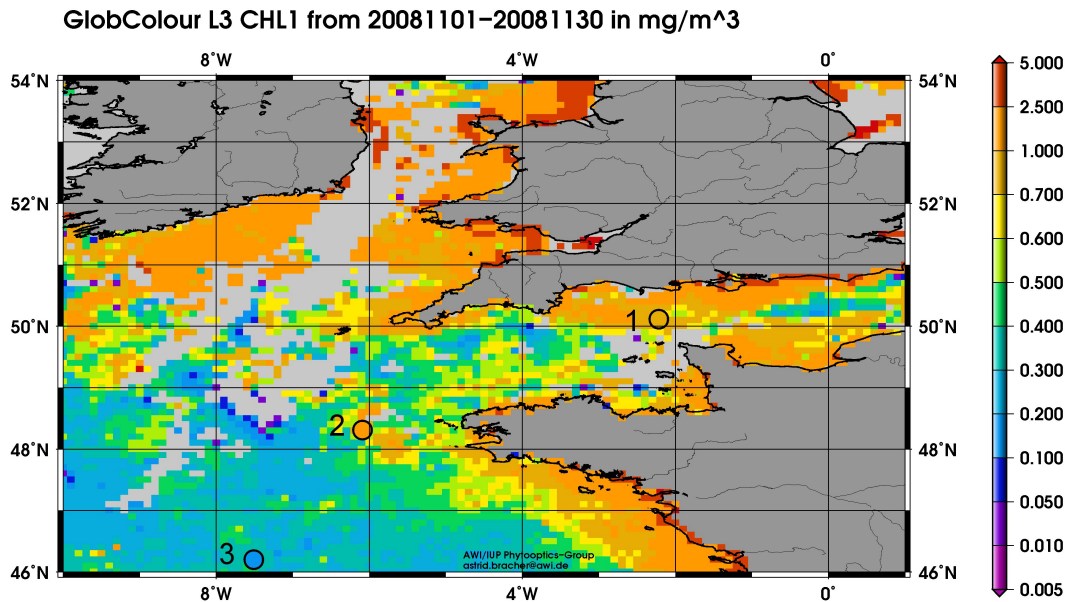


**Fig. 8.** Satellite image of the English Channel depicting Chl-a concentrations from the merged daily Full Product Set (FPS) of the GlobColour Archive as a monthly average for November 2008 with in-situ data of stations 1, 2 and 3.

Title Page

Abstract

Introduction

Conclusions

References

Tables

Figures

◀

▶

◀

▶

Back

Close

Full Screen / Esc

Printer-friendly Version

Interactive Discussion



GlobColour L3 CHL1 from 20081101–20081130 in  $\text{mg}/\text{m}^3$

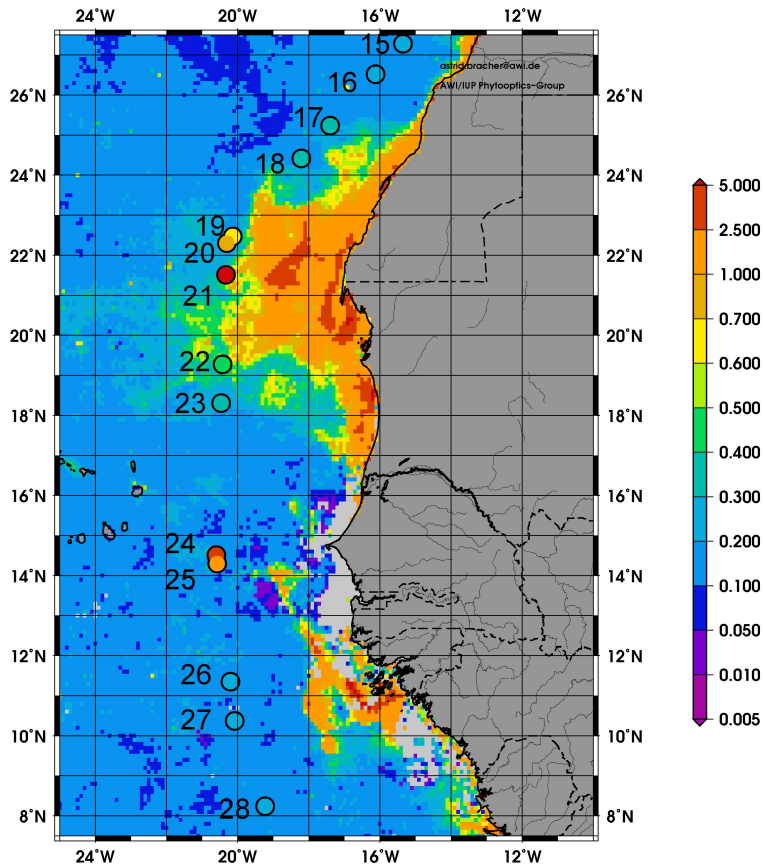


**Fig. 9.** Satellite image of the east Atlantic Ocean along the coast of North-West Africa depicting Chl-*a* concentrations from the merged daily Full Product Set (FPS) of the GlobColour Archive as a monthly average for November 2008 with in-situ data of stations 15–28.

## Bio-optical provinces in the eastern Atlantic Ocean

B. B. Taylor et al.

Title Page

Abstract

Introduction

Conclusions

References

Tables

Figures

◀

▶

◀

▶

Back

Close

Full Screen / Esc

Printer-friendly Version

Interactive Discussion